Rogue waves and analogies in optics and oceanography

John M. Dudley[1]*, *Goëry Genty*[2], *Arnaud Mussot*[3], *Amin Chabchoub*[4] and *Frédéric Dias*[5]

Abstract | Over a decade ago, an analogy was drawn between the generation of large ocean waves and the propagation of light fields in optical fibres. This analogy drove numerous experimental studies in both systems, which we review here. In optics, we focus on results arising from the use of real-time measurement techniques, whereas in oceanography we consider insights obtained from analysis of real-world ocean wave data and controlled experiments in wave tanks. This Review of the work in hydrodynamics includes results that support both nonlinear and linear interpretations of rogue wave formation in the ocean, and in optics, we also provide an overview of the emerging area of research applying the measurement techniques developed for the study of rogue waves to dissipative soliton systems. We discuss the insights gained from the analogy between the two systems and its limitations in modelling real-world ocean wave scenarios that include physical effects that go beyond a one-dimensional propagation model.

Rogue waves
Large-amplitude waves satisfying the common definition that their height from trough to crest exceeds twice the significant wave height. In optics, the definition is the same, but expressed in terms of optical intensity.

[1]*Institut FEMTO-ST, Université Bourgogne Franche-Comté CNRS UMR 6174, Besançon, France.*

[2]*Tampere University, Photonics Laboratory, Tampere, Finland.*

[3]*Université Lille, CNRS, UMR 8523, PhLAM — Physique des Lasers Atomes et Molécules, Lille, France.*

[4]*Centre for Wind, Waves and Water, School of Civil Engineering, The University of Sydney, Sydney, New South Wales, Australia.*

[5]*School of Mathematics and Statistics, University College Dublin, Belfield, Dublin, Ireland.*

**e-mail: john.dudley@univ-fcomte.fr*

https://doi.org/10.1038/s42254-019-0100-0

In nature, many complex systems show the unexpected emergence of rare and extreme events that can have a huge impact on their surrounding environment. A well-known example comes from oceanography, in which large-amplitude rogue waves have been associated with many maritime disasters. The difficulty in understanding the physical origin of these waves has made them as much a part of folklore as of science[1–4]. However, research into rogue waves has developed considerably since 2007, following the introduction of an analogy between the generation of large ocean waves and the propagation of light fields in optical fibres[5]. This analogy was made based on the observation of long-tailed statistics in experiments that studied noise in fibre supercontinuum generation, and it attracted intense interest in both optics and hydrodynamics. Many subsequent studies have explored the analogous characteristics of the two systems in more detail, with the view of clarifying the potential role of nonlinear focusing effects during wave propagation[6–12].

In optics, however, the term optical rogue wave has become widely applied to instabilities in a range of optical systems exhibiting long-tailed statistics, irrespective of the existence of a hydrodynamic analogy. In addition, the terminology rogue wave has become common, in a purely mathematical sense, to describe strongly localized solutions of certain nonlinear partial differential equations. Although nonlinear focusing has received most attention in hydrodynamic studies, the relative importance of linear and nonlinear effects in actually driving ocean rogue wave generation remains a subject of debate. A related discussion concerns the limitations of 1D models when applied to the complex oceanic environment.

In this Review, we provide an accessible overview of rogue waves in optics and hydrodynamics, the analogy between which was initially based on the suggested importance of nonlinear focusing in both domains. First, we introduce the main regime in which optical and hydrodynamic nonlinear wave propagation can be described by a common formalism. We then review results obtained in different optical and hydrodynamic systems, including results considered to have purely linear origins for rogue waves. Next, after reviewing optical phenomena that are potentially analogous to ocean wave propagation, we discuss particular cases (such as dissipative rogue waves in lasers) for which no such analogy is currently known. When considering water waves, we review studies of real-world ocean wave data and of wave-tank experiments in controlled environments.

Nonlinear focusing

Propagation models. In optics and hydrodynamics, the equations of wave propagation are simplified forms derived from Maxwell's equations and the Euler equations, respectively. In both cases, for unidirectional propagation and assuming that the underlying carrier waves are modulated by a slowly varying narrowband envelope, it is possible to derive a common mathematical formalism in the form of a nonlinear Schrödinger equation (NLSE) describing the evolution of the envelope in space and time[13–15]. In optics, the NLSE applies to an envelope

Key points

- An analogy between wave propagation on the ocean and in optical fibres has provided new insights into the physical mechanisms and dynamical features that underpin the occurrence of rogue waves.
- Real-time measurement techniques studying instabilities in fibre optics have highlighted the emergence of localized breather structures associated with nonlinear focusing, a scenario confirmed in wave-tank experiments.
- The experimental techniques developed for rogue wave measurement in optics have also yielded improved understanding of transient dynamics and dissipative soliton structures in lasers.
- Advanced analysis and hindcasting of real-world ocean wave data have revealed the central role of directionality and the superposition of random wave trains in the formation of ocean rogue waves.
- The emergence of oceanic rogue waves in the general case is likely to arise from both linear and nonlinear mechanisms to different degrees depending on the prevalent wind and sea state conditions.
- Machine learning could play a key role in future efforts to forecast and predict ocean rogue waves and to identify new areas of physical analogy and overlap between optics and hydrodynamics.

Supercontinuum
A broadband optical spectrum typically spanning from the visible to the infrared that is generated by a number of different nonlinear spectral broadening processes.

Envelope
A slowly varying function that modulates the amplitude of optical or water carrier waves.

Deep water
In hydrodynamics, deep water waves are those that propagate in water of depth d that is much greater than half their wavelength λ; that is, $d \gg \lambda/2$.

Soliton fission
The break-up of a higher-order background-free soliton into constituent fundamental soliton components due to perturbations going beyond the strict nonlinear Schrödinger equation description.

Carrier oscillations
Individual cycles of a propagating wave underneath a group or pulse envelope.

Modulation instability
Exponential growth of a weak perturbation on a continuous-wave excitation in any nonlinear system.

Akhmediev breather
A soliton on a finite background solution to the nonlinear Schrödinger equation that describes a single cycle of growth and decay along the propagation direction ξ with periodic behaviour along the time axis τ.

modulating electromagnetic carrier waves, whereas in hydrodynamics, it applies to an envelope that modulates long-crested surface gravity waves on deep water (and even on water of intermediate depth[14]).

A complete understanding of the origins of dispersion and nonlinearity in optics and hydrodynamics, and the derivations of the associated NLSEs, requires a detailed analysis of the physics specific to each system[13–18]. That said, a general physical understanding of why optical and water waves are described by the same NLSE model can be obtained by considering how the wave properties depend on the corresponding linear and nonlinear dispersion relations. For example, both systems exhibit frequency dependence of the wave speed — linear group velocity dispersion — and a nonlinear response at high amplitude that introduces a nonlinear phase on the wave envelope. The mathematical forms of these linear and nonlinear terms in the corresponding propagation equations are identical for the two systems (see BOX 1 and REFS[13–18] for details). The NLSE models the effect of group velocity dispersion and nonlinearity on a wave envelope, and, since we are interested in the mechanisms that can potentially lead to large envelope amplitudes, the equations are written for the regime in which dispersion and nonlinearity act together to support 'nonlinear focusing'.

Although the NLSE is a simplified model, it has proven very successful in describing wave evolution in a number of specific regimes in optics and hydrodynamics when the spectrum of the wave envelopes remains relatively narrow. However, the narrowband approximation of the NLSE is not valid for all scenarios, and more general equations have been derived to describe broadband propagation more accurately. In fibre optics, the most widely used is the 'generalized NLSE'[19], which includes the effect of higher-order fibre dispersion, Raman scattering and the frequency dependence of the nonlinear response associated with envelope steepening. This generalized NLSE model has been highly effective in modelling broadband propagation in optical fibre, even in the extreme case of supercontinuum generation[20].

In hydrodynamics, truncations of the full Euler equations to describe broadband propagation in deep water include the Zakharov Hamiltonian dynamical equations[21], and the higher-order spectral method formulation[22,23]. These approaches have been shown to be equivalent, at least for weak nonlinearities[24]. An additional compact form of the Zakharov equation has also been reported[25].

Extensions of the NLSE have been derived to model higher-order effects in hydrodynamics, most notably the Dysthe equation, sometimes referred to as the 'modified NLSE'[26,27]. In the context of optics–hydrodynamics analogies, the modified NLSE is particularly successful in identifying a soliton fission-like regime in hydrodynamics, equivalent to the onset dynamics of supercontinuum generation in optics[28].

Notwithstanding the need to use broadband propagation models for the most general comparison with experiments, the basic form of NLSE has remained attractive for many analytic and numerical studies because it clearly isolates the dispersive and nonlinear contributions to the dynamics, often in regimes beyond the apparent mathematical limits of its validity. Such cases include, for example, the use of the basic NLSE to qualitatively describe the propagation of pulse envelopes that are not strictly 'slowly varying' relative to the carrier oscillations[13]. Moreover, the integrability of the NLSE yields a number of analytic solutions that can be used to determine experimental initial conditions to generate prototype rogue waves in the laboratory[29].

Mechanisms and measurements. The nonlinear focusing mechanism that has received most attention in the study of rogue waves is the modulation (or Benjamin–Feir) instability. This refers to the exponential growth of a small modulation (or noise) on a continuous-wave input to the NLSE[21,30–34]. Plotting in terms of the normalized NLSE (BOX 1), we illustrate two scenarios of modulation instability corresponding to narrowband input spectra (FIG. 1a,b). The first one (FIG. 1a) is the evolution of an 'Akhmediev breather', a structure periodic in time τ that develops from an initial coherent sinusoidal modulation on a continuous wave[35]. Owing to non-ideal initial conditions (that is, a pure intensity modulation), its evolution is also periodic with propagation distance ξ, a manifestation of the Fermi–Pasta–Ulam–Tsingou recurrence phenomenon[36,37]. In contrast to this regular behaviour, the second scenario (FIG. 1b) shows the random evolution observed when the initial continuous wave is perturbed by low-amplitude noise. In this case, we see an approximate τ-periodicity at the reciprocal of the frequency of maximum amplification for the instability[29] and random breathing along ξ.

By contrast, we see qualitatively different evolution when the initial conditions consist of an incoherent field with near 100% amplitude noise, rather than a weakly perturbed continuous wave (FIG. 1c). We still see the emergence of strongly localized peaks, but with more erratic trajectories compared with FIG. 1b. Indeed, the evolution in this case is not strictly speaking a modulation instability, but is better described in terms of turbulence and the propagation of higher-order background-free solitons[38,39]. As we shall describe

Continuous wave
Also known as plane wave, this is a wave of constant amplitude or intensity.

Solitons
Coherent structures in a nonlinear dispersive system that display either stationary or recurrent behaviour with propagation, including stationary background-free sech-solitons and solitons on finite background that are also known as breathers.

Stokes wave
The surface elevation of water waves including 'bound' harmonic components, which to second order is written $\eta(t, z) = a\cos(\theta) + 1/2ka^2\cos(2\theta)$ where $\theta = kz - \omega t$ and k is the wavenumber given here for deep water.

below, all three scenarios in FIG. 1 have been studied in experiments.

Although the form of the NLSE in optics and hydrodynamics is the same, there are important differences in what the equation describes in each system. In optics, the underlying carrier wave is considered sinusoidal at frequency ω, whereas in hydrodynamics, the NLSE envelope modulates the Stokes wave, which (to second-order) contains contributions at both ω and the second harmonic 2ω[40]. In addition, even though the terminology optical wave breaking is used in an NLSE context to describe the steepening of an optical envelope from nonlinear focusing[41], optical carrier waves themselves do not 'break' or plunge as they do in hydrodynamics[42,43].

There are also important differences in measurements in each domain. Experiments in optical fibres generally measure only the time-domain envelope intensity, and information about carrier oscillations is not recorded. By contrast, measurements in hydrodynamics directly record the individual carrier wave amplitudes (although envelope information can be reconstructed straightforwardly[44]). Particular care must therefore be taken when comparing statistics between optics and hydrodynamics, because the statistics in fibre optics experiments are determined from the intensity envelope peaks, whereas the statistics of water waves are usually determined from the trough-to-crest heights (or crest heights or amplitudes) of individual waves. This is of special relevance

Box 1 | **NLSE models and typical parameters for optical and hydrodynamic rogue waves**

In fibre optics, the dimensional form of the focusing nonlinear Schrödinger equation (NLSE) is

$$i\frac{\partial A}{\partial z} + \frac{|\beta_2|}{2}\frac{\partial^2 A}{\partial T^2} + \gamma|A|^2A = 0 \quad (1)$$

where $A = A(z, T)$ is the amplitude of the envelope of the wave (with SI units $W^{1/2}$), z is the spatial coordinate, T is time, β_2 is the group velocity dispersion and γ is the nonlinearity parameter.

In hydrodynamics, the corresponding equation is

$$i\frac{\partial u}{\partial z} - \frac{1}{g}\frac{\partial^2 u}{\partial t^2} - k_0^3|u|^2u = 0 \quad (2)$$

where $u = u(z, t)$ (with SI units m) is the amplitude of the envelope of a group of deep water waves, t is time, $g = 9.81\,m\,s^{-2}$ is the acceleration due to gravity, $k_0 = 2\pi/\lambda$ is the wavevector and λ is the wavelength.

These equations can be reduced to the normalized form

$$i\frac{\partial \psi}{\partial \xi} + \frac{1}{2}\frac{\partial^2 \psi}{\partial \tau^2} + |\psi|^2\psi = 0 \quad (3)$$

where for fibre optics $\psi = A/P_0^{1/2}$, $\tau = T/T_0$ and $\xi = z/L_{NL}$, $T_0 = (|\beta_2|L_{NL})^{1/2}$ and $L_{NL} = (\gamma P_0)^{-1}$; P_0 has SI units W. For hydrodynamics, $\psi = u/u_0$, $\tau = t/T_0$, $\xi = -z/L_{NL}$, $T_0 = (2L_{NL}/g)^{1/2}$ and $L_{NL} = (k_0^3u_0^2)^{-1}$; u_0 has SI units m. Note that the carrier wavelength does not appear explicitly in the optical NLSE but is nonetheless an important parameter, determining whether the NLSE is focusing or defocusing in a particular material. In particular, focusing NLSE behaviour is observed for $\lambda_0 > 1.3\,\mu m$ in standard silica fibre and can be observed at shorter wavelengths using specialty photonic crystal fibres[13].

In the Table, we summarize typical parameters and characteristics of rogue waves.

	Fibre optics	Wave tank	Ocean
Typical parameters and physical dimensions	$\beta_2 < 0$ with $\|\beta_2\| \approx 0.1$–$20\,ps^2\,km^{-1}$; $\gamma > 0$ with $\gamma \approx 1$–$100\,W^{-1}\,km^{-1}$	$k_0 \approx 1$–$25\,m^{-1}$; $\lambda_0 \approx 6.25$–$0.25\,m$; $\omega_0 \approx 3.1$–$16\,rad\,s^{-1}$	$k_0 \approx 0.004$–$4\,m^{-1}$; $\lambda_0 \approx 1{,}600$–$1.6\,m$; $\omega_0 \approx 0.2$–$6.3\,rad\,s^{-1}$
Driven (coherent) initial conditions	Temporally modulated continuous-wave laser, shaped frequency comb, ultrashort pulses	Driving unidirectional or directional waveform sent in the time or frequency domain to paddles in a wavemaker	NA
Possible noise sources in initial conditions	Quantum noise, amplified spontaneous emission, technical laser noise	Random initial conditions sent to wavemaker	Wind, random crossing sea interactions
Typical rogue wave characteristics	Peak power $P \approx 1$ W to 10 kW, duration $\Delta\tau \approx 1$–10 ps	Wave height (trough-to-crest) $H_{max} \approx 5$ cm for period ~0.6 s and $\lambda_0 \approx 0.5$ m, $H_{max} \approx 16$ cm for period ~1 s and $\lambda_0 \approx 1.6$ m	Wave height (trough-to-crest) $H_{max} \approx 25$ m for period ~10 s and $\lambda_0 \approx 150$ m
Measurement resolution	Real time (time lens) ~220 fs; time-averaged (for instance, frequency-resolved optical gating (FROG)) <5 fs	Wave gauges: 0.002 s	Lasers: 0.1 s; buoys: 0.5 s

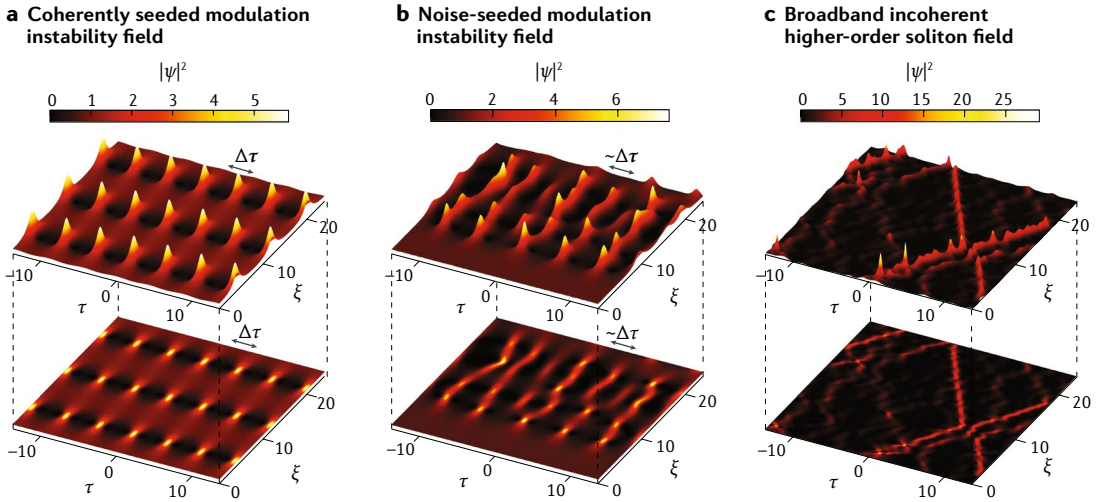

Fig. 1 | **Localization properties of nonlinear focusing dynamics in the nonlinear Schrödinger equation for three different cases. a** | 'Breathing' with propagation distance ξ of a train of localized pulses periodic in time τ. Such a train of Akhmediev breathers is generated from an initial coherent modulation on a continuous wave at $\xi = 0$, with modulation frequency at the peak of the instability gain such that the period is $\Delta\tau = \sqrt{2}\,\pi$. **b** | The complex noisy field of peaks that emerge when the continuous-wave initial condition at $\xi = 0$ is perturbed by low-amplitude broadband random noise. In this case, we see approximate periodicity with mean period $\Delta\tau \approx \sqrt{2}\,\pi$, and random breathing along ξ. **c** | The qualitatively different behaviour when the initial conditions consist of an incoherent broadband pulse rather than a continuous wave. Here we see turbulent evolution and the emergence of random higher-order background-free solitons. All plots show the space–time evolution of the intensity $|\psi|^2$ plotted above the corresponding two-dimensional projection.

to the criterion that, in oceanography, identifies a rogue wave as one whose trough-to-crest height exceeds twice the 'significant wave height' (the mean height of the highest third of waves in a measured population). In optics, although the criterion is the same, it is expressed in terms of envelope peak intensities. There are some other key differences between the two systems relating to typical design of controlled experiments, possible noise sources, measurement resolution in experiments and typical characteristics of rogue waves that have been observed. These are summarized in BOX 1.

Finally, although renewed interest in the link between optics and hydrodynamics was stimulated by the possibility of better understanding rogue waves, analogous nonlinear propagation effects had in fact been independently observed in both fields over many years. This is to be expected, given the centrality of the NLSE in describing nonlinear focusing in both environments, and the parallel development is illustrated through a timeline (FIG. 2). Some of these results will be discussed in more detail below, and more exhaustive historical treatments appear in REFS[2,11–13,45,46].

Rogue waves in optics

Overview. The 2007 proposal that an optical system could display properties mimicking oceanic rogue waves was based on noise measurements of an optical supercontinuum[5]. Specifically, a relatively new experimental technique at the time, known as the dispersive Fourier transform (DFT), was used to measure pulse-to-pulse ('shot-to-shot') fluctuations in the shape of supercontinuum spectra generated from high-power picosecond pulses injected in an optical fibre. Although it was well known that stable supercontinuum generation was possible by using femtosecond pulse pumping, the DFT measurements of a picosecond supercontinuum revealed great variations in the structure of the spectra generated from sequential pulses. Moreover, when filtering the supercontinuum spectra at long wavelengths in which (background-free) optical solitons were expected to form, the corresponding time series showed a highly asymmetric 'L-shaped' probability distribution, with a long tail containing a small population of high-intensity peaks.

A link between these spectral instabilities and ocean rogue waves was proposed, based mostly on the similarity of these long-tailed statistics to those of extreme events[47] but also on the common NLSE model for deep water waves and optical fibre propagation discussed in the previous section. The supercontinuum results immediately attracted interest and stimulated many other experiments in optics. However, the description optical rogue wave was rapidly generalized to refer to any optical system displaying long-tailed statistics, even when there was no obvious correspondence with analogous oceanic dynamics.

Although this broader usage in optics is now well established, to avoid confusion it is essential to specify when a particular experiment in optics has a potential analogy with a hydrodynamic or oceanographic system. Next, we first focus on describing one-dimensional and two-dimensional propagation experiments for which there is a potential hydrodynamic analogy. We then review the rapidly emerging field of real-time characterization of dissipative soliton instabilities in lasers. Although these laser dynamics are likely to be without a natural oceanographic equivalent, the field has developed directly from applying the real-time measurement

Significant wave height
Mean wave height from trough to crest of the upper third of all events in a recorded time series of surface elevation. In optics, the equivalent quantity is 'significant intensity', the mean intensity (from zero) of the upper third of all events in a recorded intensity time series.

Dispersive Fourier transform
Also known as time stretch and used for real-time spectroscopy, this technique temporally stretches an ultrashort pulse through linear dispersion such that its temporal intensity assumes the form of its spectrum.

Dissipative soliton
Stable localized structure that is localized as a result of balance between nonlinearity, dispersion and energy exchange (gain or loss) with an environment.

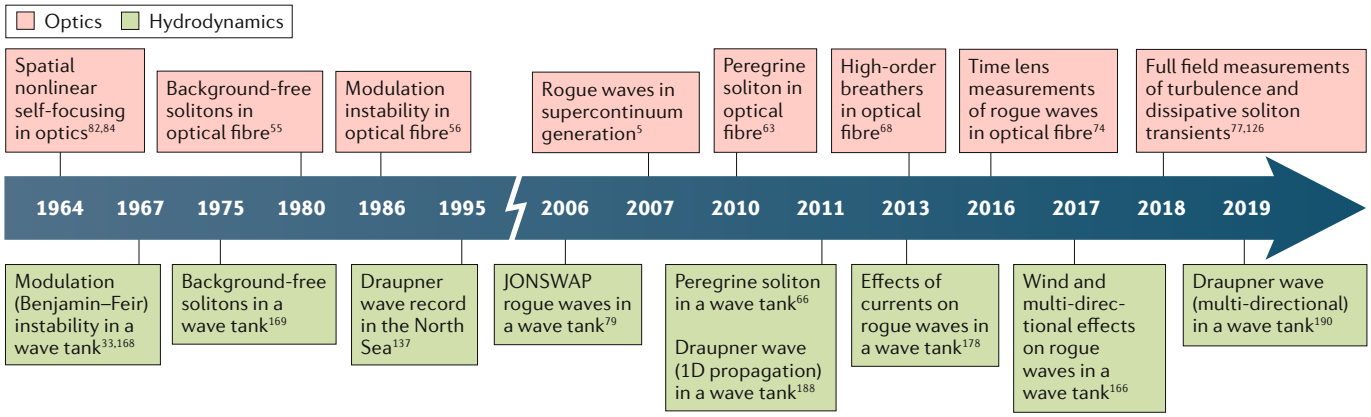

Fig. 2 | **Timeline illustrating the parallel developments in fibre optics (top) and hydrodynamics (bottom).** In hydrodynamics, we focus especially on listing a selection of wave-tank recreations of the Draupner wave because of its central place in the study of rogue waves.

techniques used for the study of rogue waves in optics, and it may stimulate studies of other classes of nonlinear dissipative structures in hydrodynamics.

One-dimensional propagation. Following the initial experiments[5] from 2007, numerical simulations were used to study the statistics and dynamics of supercontinuum rogue waves in more detail[48]. These simulations showed that the distinct solitons observed in the picosecond supercontinuum emerged from an initial phase of noise-driven modulation instability, and the shifts to longer wavelengths of the small number of 'rogue solitons' in the filtered tail of the DFT histogram arose from inelastic collisions mediated by the Raman effect[48,49]. However, although leading to long-tailed statistics, these Raman soliton dynamics appeared to be very specific to supercontinuum generation and therefore of primary relevance to the optical domain[46].

By contrast, the initial propagation phase of the modulation instability had earlier been proposed as a mechanism for hydrodynamic rogue wave generation[50–54], and attention in optics therefore quickly focused on this regime. The modulation instability and solitons in fibre optics had been studied since the 1980s, but had been characterized using only time-averaged measurements of the optical spectrum and/or the temporal intensity autocorrelation function[13,55–57]. These were the state-of-the-art characterization techniques at the time, but the development of real-time techniques such as the DFT, and the possibility of an analogy with rogue waves, motivated new experimental studies in optics.

It was particularly interesting to use optics to study nonlinearly localized analytic NLSE 'breather' structures that emerged from the modulation instability, as it had been suggested that their nonlinear growth and decay were typical characteristics of ocean rogue waves[6,58,59]. Moreover, there was additional evidence from the shape of time-averaged spectra (specifically the slope of the spectral wings) that breather structures were present in noise-driven modulation instability[60].

The first studies of nonlinear breathers in the context of rogue waves used coherently modulated fields injected into optical fibre to excite specific analytic solutions (FIG. 1a). Because of the coherent seeding, the excited breathers were stable, and did not require real-time characterization. Rather, it was possible to use averaging techniques such as frequency-resolved optical gating[61] or optical sampling[62] to record the breather profiles. These experiments characterized a range of nonlinear structures, including the Akhmediev breather, the Peregrine soliton and the Kuznetsov–Ma soliton[63–65], and were important in motivating studies in hydrodynamic wave tanks as described below[66].

The comparison of these measurements with analytic predictions was particularly important in showing that an optical fibre system, before the onset of supercontinuum generation, could be considered as a close-to-ideal NLSE environment. Additional experiments coherently exciting higher-order breather solutions of the NLSE further supported this interpretation[67–69]. Related experiments extended the study of hydrodynamic analogies in optics even further, reporting controlled shock dynamics[70] and dam-breaking phenomena[71,72].

Although impressive in showing the ability of an NLSE system to support nonlinear localization, the direct relevance of optical experiments using coherent initial conditions to noise-driven rogue waves on the ocean remained unclear. Certainly, numerical studies of noise-driven modulation instability show the emergence of random localized structures (FIG. 1b), and a detailed study of the intensity profiles showed that they cluster around the analytic breather solutions of the NLSE (REF.[73]). The key question, however, was whether these could be measured. Such experiments appeared challenging, requiring the measurement of real-time temporal profiles with subpicosecond resolution, much shorter than the response time of available photodetectors.

To this end, new experimental techniques were developed[38,74]. The idea is to transpose the action of an optical lens that magnifies an object in space, to temporally stretch noisy picosecond structures from the modulation instability to nanosecond duration replicas that could be measured (in real time) using high-speed photodetectors (FIG. 3A). Such a 'time lens' exploits the mathematical equivalence of paraxial diffraction in space and linear group velocity dispersion in time[75], and combines two

Peregrine soliton
A limiting case of the Akhmediev breather and Kuznetsov–Ma soliton solutions that is doubly localized along the propagation direction ξ and τ.

Kuznetsov–Ma soliton
A soliton on a finite background solution to the NLSE describing periodic oscillation along the propagation direction ξ with localization along τ.

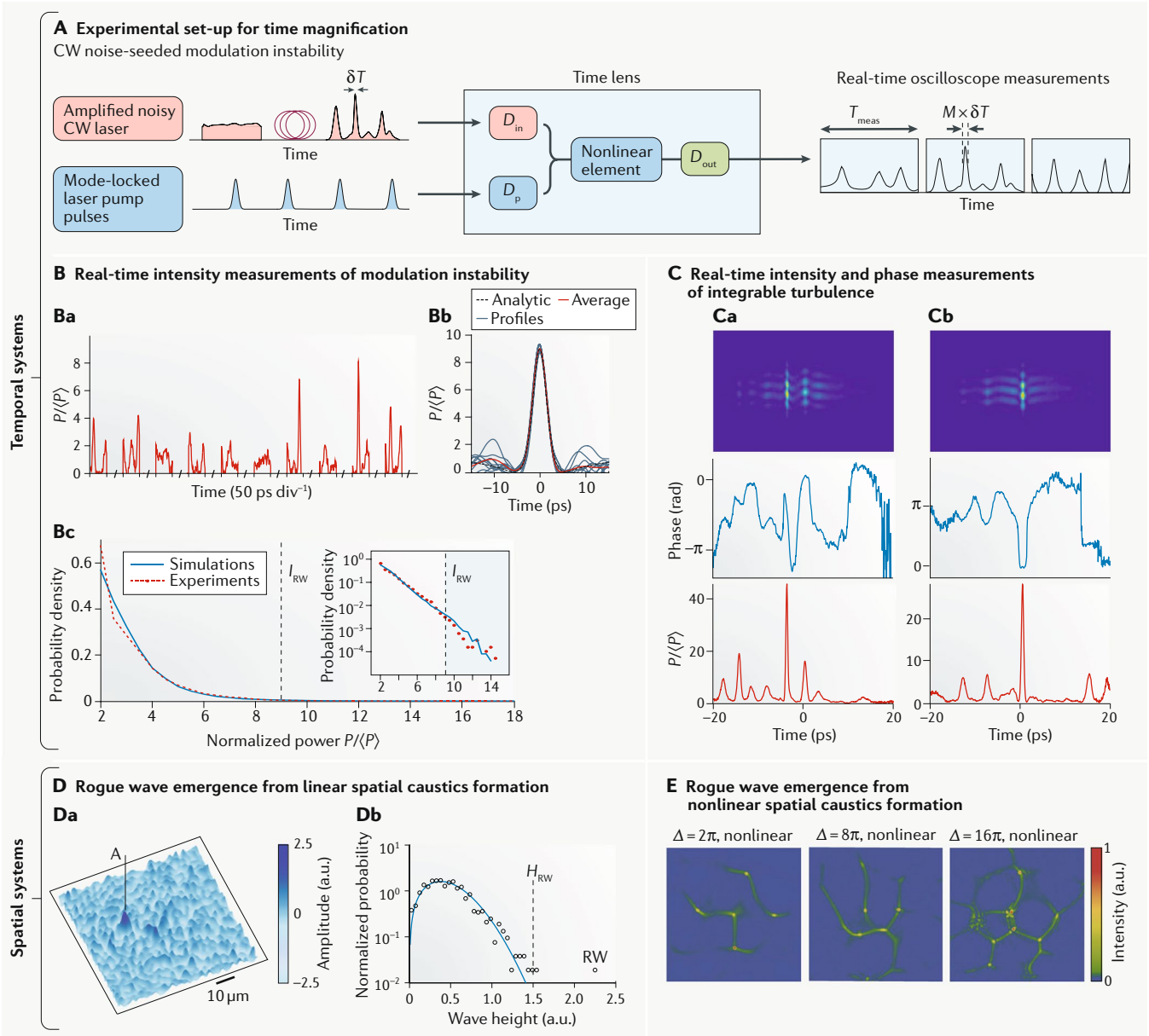

Fig. 3 | **Optical rogue wave measurements. A** | Schematic for temporal magnification of random modulation instability generated by a noisy continuous-wave (CW) laser injected into optical fibre. Pulses from a mode-locked laser develop a quadratic temporal phase after dispersive propagation D_p before being combined with the dispersed modulation instability signal in a nonlinear element (waveguide or crystal). The nonlinear element transfers the pump quadratic phase to the modulation instability signal such that another dispersive propagation step yields time-magnification by a factor $M = |D_{out}/D_{in}|$ where D_{in} and D_{out} are the dispersion parameters before and after the nonlinear element. **B** | Real-time measurements of breather dynamics emerging from noise-seeded modulation instability. Sequential windows of breather intensity profiles normalized with respect to the average output background power $\langle P \rangle$ and rescaled to account for temporal magnification (panel **Ba**). The measurement window T_{meas} is determined by the mode-locked pulses (note the broken axis between measurements, each 50 ps long; div, division). Superposed experimental breather profiles (grey lines), comparing their average (red line) with the analytic Peregrine soliton (black dashed line) (panel **Bb**). Long-tailed normalized probability density of random modulation instability breather peaks, comparing experiments (red) and simulations (blue) (panel **Bc**). The inset uses semi-logarithmic axes. The calculated rogue wave intensity threshold (I_{RW}) is shown as a dashed black line. **C** | Real-time complex field (intensity and phase) of integrable turbulence dynamics generated by nonlinear fibre propagation of a broadband noisy input field with near-100% contrast. Two typical measurements (panel **Ca**, **Cb**) using a time-lens set-up with the addition of heterodyne detection for phase retrieval. Each subpanel shows typical raw images captured by the set-up (top panels), the retrieved phase (middle panels) and intensity (bottom panels). <*P*> is the output background power. **D** | Rogue wave statistics in a purely linear optical system due to caustic focusing of a spatial field with random phase. Measured spatial amplitude (panel **Da**) of the electric field when the initially applied random phase yields a spatial spectrum intermediate between that of a partially developed speckle and a caustic network. The trough-to-crest statistics (panel **Db**) are near-Rayleigh distributed (fit shown as the blue solid line) with an extended tail including rogue wave (RW) events exceeding the significant wave height (H_{RW}). The bright peak A labelled in panel **Da** is the highest peak observed in the distribution. **E** | Typical caustic networks observed during spatial rogue wave generation in a rubidium cell via nonlinear amplification of initial small phase fluctuations. Δ, amplitude of the random phase. Panel **B** is adapted from REF.[74], CC-BY-4.0 (https://creativecommons.org/licenses/by/4.0/). Panel **C** is adapted from REF.[77], Springer Nature Limited. Panel **D** is adapted from REF.[99], CC-BY-4.0 (https://creativecommons.org/licenses/by/4.0/). Panel **E** is adapted with permission from REF.[102], APS.

segments of dispersive propagation on either side of a time lens element that introduces a temporal quadratic phase[76]. The addition of a supplementary heterodyne detection stage can also be used to yield intensity and phase information[77].

Experiments using time-lens techniques have studied noise-seeded NLSE propagation in optical fibre (FIG. 3B,C). The use of a narrowband noisy continuous-wave input revealed the emergence of random localized structures (FIG. 3Ba), with intensity profiles well fitted by analytic NLSE breather solutions[74] (FIG. 3Bb). The measurement of a large dataset also allowed the intensity statistics of the modulation instability peaks to be directly characterized (FIG. 3Bc), confirming the expected highly asymmetric probability distribution[73]. These results highlighted the role of breather collisions (or higher-order breathers[67,68]) in generating the largest intensity events that satisfied statistical criteria to be identified as rogue waves (events above the rogue wave intensity I_{RW}).

Using a heterodyne time lens, the intensity and phase of spontaneous structures were measured in the turbulent regime excited by an incoherent input field with near 100% intensity fluctuations[77] (FIG. 3C). In this case, the dynamics are described in terms of incoherent higher-order background-free solitons (FIG. 1c). Long-tailed intensity statistics were also observed in the same study[77] and were important in confirming that spontaneous rogue-wave like statistical behaviour could be observed with large initial fluctuations beyond the scenario of modulation instability. Earlier results in a similar turbulent regime[38] were also notable for showing how the temporal compression seen during incoherent higher-order soliton propagation led to the emergence of the Peregrine soliton, a remarkable result that was later confirmed using coherent initial excitation[78]. These experiments also motivated follow-up work to tailor the incoherent optical input spectrum to match a scaled version of the Joint North Sea Wave Project (JONSWAP) spectrum for ocean waves[79]. A quantitative comparison between the scaled statistics obtained in optics and those from measurements in a 1D wave tank showed good agreement[80]. Experiments have also been performed by exciting modulation instability from noise in a regime in which the expected ~100 ps timescale of nonlinear localization falls within the bandwidth of direct high-speed detection[81]. By using a new recirculation loop set-up, it was possible to measure the space–time development of modulation instability over an extended propagation distance, directly revealing the expected multiple recurrence cycles and incoherent evolution dynamics (see also FIG. 1b and REF.[73]).

Two-dimensional propagation. We have so far described optical fibre experiments studying nonlinear focusing dynamics in the time domain, analogous to 1D wave propagation on deep water. It is important to note, however, that the first studies of nonlinear focusing in optics were carried out in the spatial domain[32,82,83], motivated by the unexpected damage observed when the first lasers were focused into glass[84]. More systematic experiments in controlled 1D geometries reported soliton behaviour in free space and waveguide systems[85,86], and optical spatial solitons in general exhibit a rich landscape of nonlinear interactions[87].

It is thus unsurprising that early studies of rogue waves in optics also considered nonlinear spatial instabilities[88–91], but the nonlinear optical systems used in these experiments were such that no simple analogy with an equivalent hydrodynamic scenario could be drawn. However, studies of higher-dimensional wave propagation on the ocean (involving short-crested waves) have shown that nonlinearity is not a requirement to see rogue-wave like behaviour. Rogue waves in the ocean have also been attributed to the linear superposition of random waves propagating in different directions[92], linear and nonlinear caustic formation[93,94], and linear directional focusing[95,96].

In optics, experiments on linear wave-shaping mechanisms in the spatial domain have been performed by studying laser speckle. Laser speckle is the granular intensity distribution that arises from the spatial interference of a large number of coherent wavefronts with random phases[97] and is known to exhibit long-tailed statistical properties[98]. To study the potential link between speckle and rogue waves, the experiments in REF.[99] imprinted a random phase pattern on the transverse profile of a laser beam, and the variation in the beam profile was then characterized during linear propagation (diffraction) in air. With sufficient propagation, the random initial phase was converted into amplitude fluctuations across the transverse profile and, by using phase retrieval techniques, it was possible to determine the statistics of both the spatial amplitude and intensity. By controlling the strength of the initial random phase, the far-field intensity pattern could be varied from partially developed speckle to a broadband caustic network[100]. In this case, a long-tailed distribution was observed with a considerable fraction of rogue waves. In an intermediate range of initial phase fluctuations, it was possible to synthesize an 'optical sea' in which the spatial amplitude statistics followed a Rayleigh distribution but still showed the presence of a small fraction of events above the rogue wave threshold[99] (FIG. 3D). These results were important in explicitly confirming the possibility of seeing rogue wave statistics from purely linear propagation in an optical system, displaying a clear analogy with ocean wave superposition. Theoretical work has also shown that rogue waves can arise from purely linear superposition in a 1D environment for a sufficiently large number of random interacting data bits in an optical communications channel[101].

A follow-up experiment studying optical caustics (with random phase fluctuations as initial conditions) replaced linear propagation in air with nonlinear propagation in a gas cell described by a 2D NLSE model[102]. In this case, experiments showed that nonlinearity enhanced the generation of high-intensity caustics on the transverse beam profile (FIG. 3E). Importantly, these results showed that nonlinearity could enhance the generation of high-intensity events whose initial origin was due to a linear propagation effect. This underlines the fact that, in the optics domain, both linear and nonlinear focusing can combine to generate rogue waves.

Long-tailed distribution
A characteristic of statistical distributions in which the tails decrease very slowly and contain a subpopulation of extreme events.

Mode-locked lasers
Lasers typically emitting picosecond-duration or femtosecond-duration pulses as a result of either active or passive phase synchronization of the longitudinal modes of the laser cavity.

Coherence
Phase stability of carrier oscillations of a single frequency wave, or the stability of the phase difference between the carrier oscillations of two waves.

Transient instabilities in lasers. In addition to the experiments described above for which a close analogy exists with ocean waves, research has also developed in an area in which no such analogy has yet been found: the characterization of ultrafast transient instabilities in mode-locked lasers. Although stable mode-locked lasers are well known to produce highly regular pulse trains, they can also show complex behaviour during their start-up dynamics or when detuned from steady state[103]. Moreover, the past few years have seen mode-locked laser instabilities described in terms of dissipative soliton theory, in which the concept of a localized soliton is generalized from solely the balance between dispersion and nonlinearity to include dissipation in the form of gain and loss[104]. This led to the description of extreme instabilities in such lasers as dissipative rogue waves[105].

Following the 2007 optical rogue wave experiments in fibre[5], experiments using pulse energy measurements showed that mode-locked lasers could also exhibit long-tailed statistics[106,107]. The real-time DFT technique was also used to study fibre laser spectral instabilities[108], yielding measurements of a new soliton collapse and recovery (or 'explosion') regime[109,110] (FIG. 4A). Interestingly, earlier photodiode measurements and experiments with frequency-resolved optical gating[111] or single-shot spectral characterization[112] had reported signatures of complex instabilities in mode-locked lasers, but the availability of the DFT and time-lens techniques renewed interest in this field.

Studies were also performed on the soliton build-up dynamics in a Kerr-lens mode-locked Ti:sapphire laser[113]. Using a modified DFT method for real-time spectral interferometry, soliton bound states can be characterized[114] (FIG. 4B). Many other experiments have used the DFT technique to study evolving soliton dynamics and multi-pulse states[115–122], and intensity and coherence measurements in partial and coherent mode-locking regimes[123]. An example of dissipative soliton formation in a polarization rotation mode-locked fibre laser[124] is shown in FIG. 4C. A particular advantage of real-time spectral measurements is that it allows complementary information on temporal soliton separation to be determined through the associated field autocorrelation (FIG. 4B,C).

Combining real-time spectral characterization using DFT and high-speed measurements using photodiodes enabled the study of a range of multi-scale dynamics in a mode-locked fibre lasers[125]. By combining the DFT with the time-lens technique, simultaneous measurement of spectral and temporal profiles was possible with sub-nanometre and subpicosecond resolution. These experiments yielded a complete picture of the unstable start-up dynamics of dissipative solitons in a mode-locked fibre laser[126], with typical results showing the growth and collapse of a temporal multi-soliton complex (FIG. 4DA). Moreover, with the simultaneous measurement of spectral and temporal intensity profiles, the use of phase retrieval techniques allowed the reconstruction of the full field (in amplitude and phase) of the evolving solitons (FIG. 4DB). In addition to studying mode-locked lasers, real-time techniques have been applied to study related soliton dynamics in other dissipative systems such as microresonators[127,128].

Rogue waves in oceanography

Overview. Although stories of unexpected large ocean waves date back to antiquity, it was only in the twentieth century that any comprehensive scientific study of their properties began[2]. Several catalogues of records of rogue waves are now providing insights into the long history of attempts to record their occurrence as distinct oceanic events and to understand their properties[129–133]. The description of such events as freak waves was apparently first used in the scientific literature in 1964 (REF.[134]), although this terminology was found in newspaper accounts even earlier[135]. The alternative and now more common name rogue wave first seems to have appeared in a 1962 novel by C. S. Forester[136]. Despite being a work of fiction, it gives a remarkably clear physical description of "the 'rogue wave', generated by some unusual combination of wind and water".

It is generally accepted that the systematic study of rogue waves began with the milestone experimental measurement, on 1 January 1995, of a wave with trough-to-crest height of 25.6 m on the uncrewed Draupner E oil platform in the North Sea[137]. The fact that this Draupner (or New Year's) wave was observed within an extended time series at high-sampling frequency yielded great confidence in the measurement fidelity and stimulated the oceanographic community to investigate the physics and statistics of ocean rogue waves on a quantitative level.

The environment of the open sea involves multiple physical processes such as currents, dissipation, wind forcing and wave breaking. Aside from wave breaking, which is by nature nonlinear, currents, dissipation and wind forcing can be either linear or nonlinear. Despite this complexity, however, it has been possible to describe many aspects of large-amplitude ocean wave dynamics in regimes in which the physics is dominated by particular distinct linear or nonlinear mechanisms. For example, the linear processes of random wave superposition[92] and dispersive focusing[138] are both well-understood mechanisms that can lead to increased wave amplitude, and nonlinear focusing from modulation instability has been particularly studied because of its driving influence on wave localization and decay[21,30–34]. It is important to note, however, that although nonlinear focusing has certainly attracted much attention in the context of ocean rogue wave formation, determining the relative contribution of linear and nonlinear effects in driving rogue wave dynamics remains a subject of much study[12,139].

Rogue waves in the natural environment. Because rogue waves are rare events with sudden growth and decay dynamics, their measurement is extremely challenging, requiring both long time series (over months or even years) to capture their rarity, and a sampling frequency between 2 Hz and 10 Hz to record the main features of wave shapes. The most reliable rogue wave measurements are based on the reflection of an optical or acoustic signal at the boundary between sea and air[2]. The 1995 Draupner wave, for example, was recorded by a laser sensor using a sampling frequency of 2.13 Hz during 20 minutes of every hour. A similar technique was used to record a second landmark measurement of what is known as the Andrea wave. It was measured

on 9 November 2007 in the North Sea with a sampling frequency of 5 Hz during 20 minute intervals by four independent lasers mounted on the Ekofisk platform[140]. Related measurement techniques include using a mounted microwave radar[141] and acoustic Doppler current profilers[142].

Other methods for measuring rogue waves have been reported, but there has been debate over their fidelity.

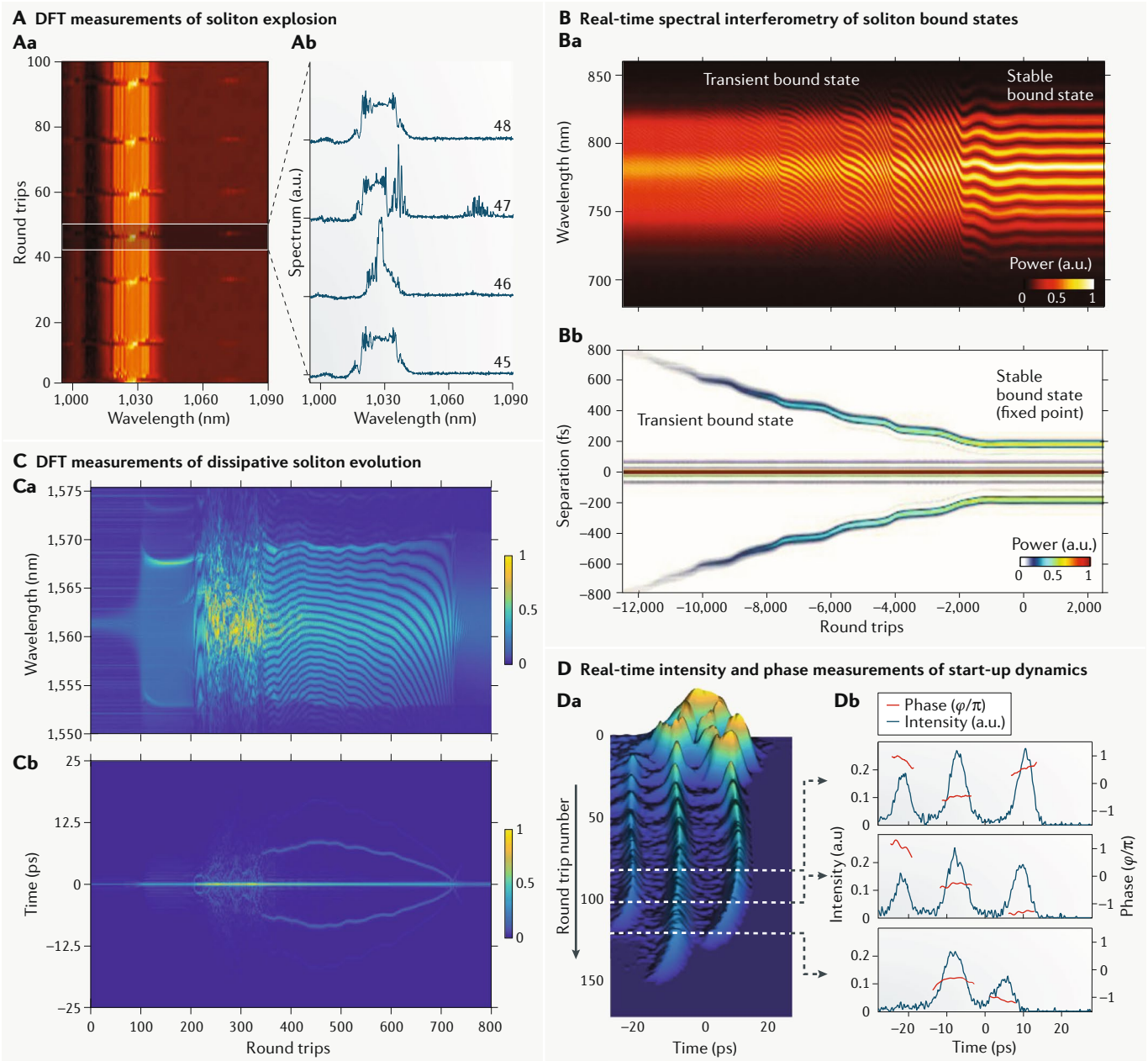

Fig. 4 | **Characterization of transient instabilities in lasers. A** | Dissipative soliton explosions in an Yb-doped mode-locked fibre laser operating in the transition regime between stable mode-locking and noise-like emission. Experimental single-shot spectra of 100 round trips showing several explosion events (panel **Aa**). A close-up of the explosion dynamics shows that the spectrally broad soliton collapses into a narrower spectrum with higher amplitude before recovering to its previous state (panel **Ab**). **B** | Soliton bound states in a few-cycle mode-locked laser. Real-time interferogram (panel **Ba**) of 15,000 consecutive cavity round trips shows soliton bound-state formation with locked phases. Field autocorrelation evolution over the 15,000 round trips (panel **Bb**) shows reduction of the soliton temporal separation to form a stable bound state. **C** | Formation of coherent dissipative soliton structures from unstable noise in nonlinear polarization rotation mode-locked fibre laser. The real-time spectral evolution (panel **Ca**) of the laser output during dissipative soliton build-up is measured with dispersive Fourier transform (DFT). The field autocorrelation evolution over 800 round trips (panel **Cb**) traces the evolution of the temporal separation between the dissipative solitons. **D** | Dissipative soliton dynamics during start-up phase of a passively mode-locked Er-fibre laser. Temporal evolution over 170 round trips (panel **Da**) captured using a time-lens system shows growth and decay of multiple dissipative soliton structures as the laser passes through a transient unstable regime before stable mode-locking. Plots (panel **Db**) showing the full field (intensity in blue-black and phase in red) reconstructed from simultaneous dispersive Fourier transform and time-lens measurements correspond to specific round trips as indicated. Panel **A** is adapted with permission from REF.[109], OSA. Panel **B** is adapted with permission from REF.[114], AAAS. Panel **C** is adapted from REF.[124]., CC-BY-4.0 (https://creativecommons.org/licenses/by/4.0/). Panel **D** is adapted from REF.[126], Springer Nature Ltd.

For example, measurements relying on accelerometers placed on wave buoys can exhibit distortion due to the buoy's intrinsic moment of inertia[2], despite a number of rogue wave events have been extracted from buoy measurements using appropriate quality control[143–146]. Moreover, most measurements have been limited in the information they can yield about rogue wave properties because they record time series only at the single point where the sensor is located.

Improved approaches to satellite remote sensing continue to be explored[147]. Techniques such as stereo video are also promising as they can capture the space–time evolution of the sea surface over an extended region[148,149]. There has also been considerable interest in remote sensing with satellite-based synthetic aperture radar[150], but such imagery is associated with errors due to velocity bunching and azimuthal image smear[151]. Nonetheless, there is emerging consensus that recording the full spatiotemporal evolution of waves (both long-crested and short-crested waves) on the ocean's surface is essential to fully characterize the statistics of large waves in complex sea states, such as hurricanes and storms. This is because the maximum height of a group of waves propagating in a complex manner over a large area during a given time interval is likely to be greater than the wave height observed at only one fixed point in space (as measured by, for example, a moored buoy). The study of such a 'space–time extreme' is an important current area of research[149,152].

Despite the challenges of measurement, appropriate quality control has been applied to many extended time series of wave records, and potentially thousands of candidate rogue waves have been identified. There are several earlier reviews of rogue waves in oceanic and coastal environments[2,3]; a summary of results from fixed platforms and an analysis of a large dataset of wave buoy data has appeared in REF.[146]. A particular conclusion of these recent summaries was that mechanisms for rogue wave formation vary from place to place in the ocean.

Hindcasting simulations. The characteristics of several large ocean wave events have also been analysed in detail using an approach known as hindcasting. Such studies use archived meteorological and wave data at the location of the event under study to determine initial conditions for a forward-propagating wave model[153]. The aim is to use the model to simulate the wave-field characteristics at later times and compare them quantitatively with a measured wave record. By varying the initial conditions and parameters of the model (particularly the directional wave energy spectrum), it is possible to draw conclusions as to which processes may be responsible for the emergence of the observed rogue waves. Studies of this type include the analysis of the maritime accidents of the fishing boat *Suwa-Maru*[154], the cruise ship *Louis Majesty*[155], the tanker *Prestige*[156], the merchant vessel *El Faro*[152], and modelling of the Draupner and Andrea waves[157,158] and rogue waves generated during Typhoon Lupit in 2009 (REF.[159]). As an example, we illustrate the case of the Andrea wave and its modelled profile using the hindcasting approach (FIG. 5A).

These studies of individual examples of real-world ocean waves have highlighted the difficulty in identifying a single primary cause for the wave enhancement, because different approaches to analysing the same event can yield different conclusions. For example, motivated in part by the presence of crossing sea states at the time of the Draupner wave, the analysis in REF.[160] initially suggested that third-order nonlinear focusing (modulation instability) in crossing seas may be important in rogue wave formation. But a further analysis and direct numerical modelling of the Draupner wave with and without the cubic nonlinear term in simulations showed that such third-order nonlinear focusing was negligible[157]. In this analysis, the wave shaping was found to be dominated by directional superposition, with a minor enhancement from the second-order bound (Stokes) nonlinear contribution. A similar conclusion can be drawn for the Andrea wave (FIG. 5A) and a negligible role for third-order nonlinear focusing was identified from the hindcasting analysis in REF.[156] considering the wave conditions associated with the Prestige accident.

Similar results were reported in REF.[161] in a study of 2 million wave groups in which 300 rogue waves were identified. Although the nonlinear modulation instability is discussed as a possible effect that can increase the wave envelope steepness, the conclusion (based on the symmetric shape of the wave groups) was that the random superposition of the Stokes waves was sufficient to explain the observations of individual rogue waves. On the one hand, results from several other groups have independently supported the interpretation that downplays the role of the modulation instability and instead highlights the role of linear interference and/or localized dispersive focusing[141,149]. On the other hand, the hindcasting analysis of rogue waves observed during Typhoon Lupit suggested that a focusing nonlinearity played a role in some instances of rogue wave formation[159].

All these various results taken together suggest that the complexity of the ocean coupled with the relatively limited observational data prevents a definitive conclusion concerning the underlying physics of ocean rogue wave formation. And, as we discuss below, in the context of laboratory experiments, both linear and nonlinear processes remain actively investigated as potential driving mechanisms for rogue waves. In this regard, it is interesting to search for convenient statistical signatures (in both simulation and real-world wave data sets) that may allow us to disentangle the role played by linear and nonlinear processes. The fourth-order moment (kurtosis) is of particular interest as it has been shown to provide a robust measure of the strength of the tails of a skewed wave height distribution[162–164].

Wave-tank experiments. Reproducing extreme wave propagation in laboratory wave tanks has been important in allowing comparisons to be made with theory and modelling under controlled conditions. For wave-tank experiments to have relevance to ocean wave dynamics, the experimental conditions should mimic the natural processes as much as possible. State-of-the-art

Long-crested and short-crested waves
The crest of a wave is equivalent to its transverse extent, with ocean waves classified as long-crested or short-crested respectively depending on whether they predominantly propagate in one direction or consist of a superposition of waves propagating in different directions.

Space–time extreme
The maximum wave surface height observed over a given area during a time interval, and not just at a given point.

Hindcasting
Also known as backtesting, an approach used to test a mathematical model by predicting wave elevation properties based on archival inputs such as directional wave energy spectra at an earlier time and comparing this with known results.

Directional wave energy spectrum
The distribution of wave energy in frequency and direction, often used to provide initial conditions for multi-dimensional linear and nonlinear wave modelling.

Crossing seas
A sea state with two independent wave systems travelling at oblique angles.

Steepness
For water waves only, the steepness is given by $ka = 2\pi a/\lambda$ where k is the wavenumber, λ the wavelength and a the amplitude.

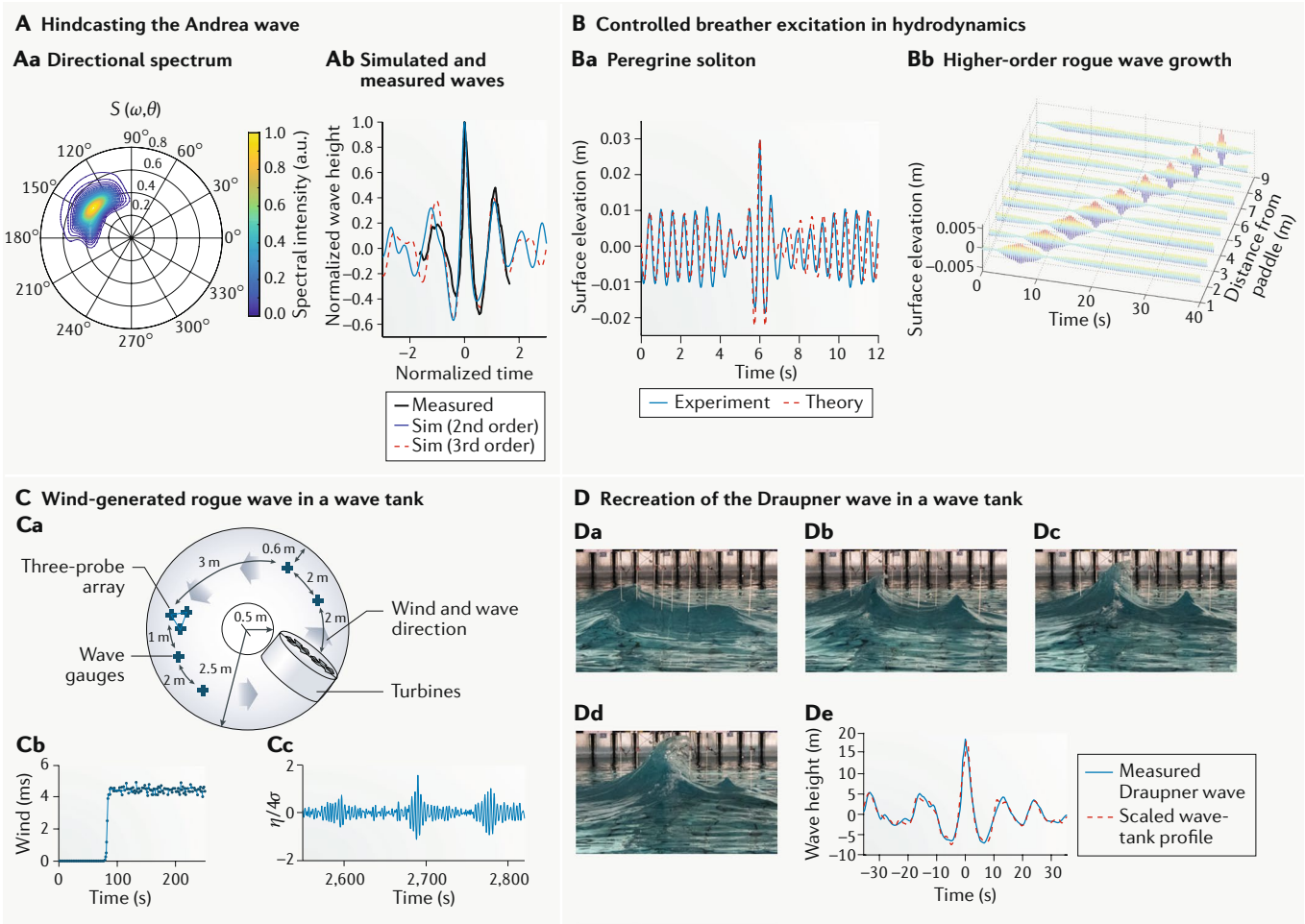

Fig. 5 | **Ocean and wave-tank measurements of rogue waves. A** | Hindcasting results for the Andrea wave. The directional wave energy spectrum $S(\omega,\theta)$ is used in numerical simulations, where ω is angular frequency and θ is direction in degrees (panel **Aa**). The measured Andrea wave (black) is compared with simulations including up to second-order (blue) and third-order contributions (red) (panel **Ab**). The minor differences between the simulations point to a negligible role from third-order nonlinear focusing. **B** | Controlled breather generation in wave tanks using initial conditions in amplitude and phase determined from analytic breather solutions to the nonlinear Schrödinger equation. Experimental (blue) Peregrine soliton is compared with the analytic prediction (red) (panel **Ba**). The evolution of a higher-order breather solution to the nonlinear Schrödinger equation is measured in a wave tank (panel **Bb**). **C** | Wind-generated waves in an annular wave tank: schematic of the elements of the experimental set-up (panel **Ca**); example of wind-speed profile used for wave generation (panel **Cb**); example of measured water surface elevation ($\eta/4\sigma$, that is, normalized to 4 times the standard deviation σ of the 10 minute record) (panel **Cc**). The wave record shown includes a rogue wave of height 2.7 times as high as the associated significant wave height. **D** | Recreation of the Draupner wave in a circular wave tank for crossing seas with a crossing angle of 120°. Images are shown of the free surface taken at intervals of 100 ms (panel **Da**–**Dd**). The scaled wave-tank reproduction (red) is compared with the measurements at the Draupner platform (black) (panel **De**). Panel **A** is adapted from REF.[157], CC-BY-4.0 (https://creativecommons.org/licenses/by/4.0/). Panel **B** is adapted from REF.[66], CC-BY-3.0 (https://creativecommons.org/licenses/by/3.0/) and with permission from REF.[174], APS. Panel **C** is adapted with permission from REF.[166], APS. Panel **D** is adapted from REF.[190] CC-BY-4.0 (https://creativecommons.org/licenses/by/4.0/).

wavemakers can be conveniently programmed to generate a wide range of initial conditions, and, with artifacts due to effects such as reflection and viscosity well understood, it is possible to use wave tanks to study many different propagation scenarios in deep or shallow water of constant or varying depth. Although many experiments on 1D propagation can be performed in narrow channels or flumes, the use of wave-making panels on the perimeter of larger wave basins, or the use of circular wave tanks, is now enabling the study of multi-dimensional effects[165]. Another geometry developed for wave-tank experiments is the annular flume, which can allow the study of some wave generation phenomena through circular propagation under essentially unlimited distance (fetch)[166].

The first use of wave tanks to study modulation instability actually arose from an experiment that went wrong[167]. Aiming to test the stability of small-amplitude water waves experimentally, T. Brooke Benjamin and Jim E. Feir unexpectedly observed the exponentially growing amplitude modulation of the wave train[168]. Following this pioneering work, other wave-tank

Shallow water
In hydrodynamics, shallow water waves are those that propagate in water of depth d that is much less than half their wavelength λ, that is, $d \ll \lambda/2$. The intermediate depth regime lies between that of shallow and deep water.

experiments investigated related deep-water (focusing nonlinearity) propagation effects such as Fermi–Pasta–Ulam–Tsingou recurrence, the emergence of strongly modulated wavepackets and the formation of isolated NLSE solitons[169–171]. Later experiments examined the effect of wave breaking, with particular emphasis on how breaking influences the long-time evolution of an evolving wave train[172,173]. Following the first observation of the Peregrine soliton in optics, there was renewed interest in studying analytic breather solutions to the NLSE in wave tanks with suitably tailored initial conditions. This led to a number of experiments reporting similar Peregrine soliton dynamics[66], and higher-order breathers[174] (see FIG. 5Ba,Bb, respectively). An additional study even generated a Peregrine soliton and examined its interaction with a model of a chemical tanker in a seakeeping test[175].

An important experiment looked specifically at how rogue waves could be triggered randomly, by driving a wavemaker with scaled initial conditions replicating the experimental JONSWAP spectrum of waves on the North Sea[79]. The experimental results were consistent with the emergence of localized NLSE breathers from the modulation instability. These results supported earlier numerical studies that had predicted that the modulation instability would increase the probability of rogue waves in random oceanic sea states[176], although the authors noted the limitation of their work in that it considered only 1D dynamics. These wave-tank experiments have been confirmed by using larger statistical data sets in recent experiments in optics, in which the optical initial conditions were tailored and scaled to match the JONSWAP spectrum parameters used in the wave-tank experiments[80]. In a related experiment, a possible rogue wave triggering effect was demonstrated in a wave tank by adding a coherent Peregrine soliton state to a random JONSWAP wave spectrum as initial conditions to a wavemaker[177].

Other works aimed to include processes found in the natural environment in wave-tank experiments. For example, studies have shown that the modulation instability and Peregrine soliton evolution can persist or even be enhanced in the presence of opposing currents[178,179]. In other experiments, the effect of wind on rogue wave dynamics has been studied in specially adapted wind–sea wave tanks[180]. Experiments in a 1D wave tank have shown that wind can induce frequency downshifting in the spectrum of initial breather solutions excited by a wavemaker[181,182], whereas other experiments in an annular wave tank did not use any initial mechanical wave generation but allowed waves to develop spontaneously from the action of the wind on the water surface[166] (FIG. 5C). These results show that wind forcing could indeed generate conditions for the observation of non-Gaussian long-tailed wave height statistics. Another work has examined the combination of nonlinear focusing with multi-dimensional effects in a wave-tank experiment using initial conditions that generated a coherent modulation envelope propagating at an angle to the carrier plane waves. These results have shown the generation of slanted solitons and breathers on the water surface, confirming that soliton-like nonlinear localization can be preserved in the presence of higher-dimensional propagation[183].

In addition to studies that explicitly set out to examine the role of the modulation instability and related nonlinear focusing on rogue wave dynamics, experiments have shown that linear dispersive focusing can also generate large-amplitude waves. Indeed, the generation of multi-frequency initial conditions with phases adjusted to lead to a focused wave group at a prescribed distance in the wave tank has been used in a number of experiments studying wave-breaking effects from large-amplitude waves[184–187]. In this context, we mention a 1D wave-tank experiment that was able to use deterministic linear superposition of component waves to reproduce a scale model of the single-position wave train of the Draupner wave[188]. Progress has also been made in understanding the role of linear and nonlinear focusing in directional seas[189], including a recent experiment recreating the Draupner wave from a multi-directional superposition[190] (FIG. 5D).

Outlook

In the past decade, there have been many examples of mutually beneficial studies of rogue waves in optics and hydrodynamics.

A particular focus of the latest studies has been the relative contributions of linear and nonlinear effects in driving the emergence of rogue waves. However, although nonlinear focusing has been shown to be a dominant mechanism of rogue wave formation in wave tanks, it has not been possible to draw the same conclusion in the more complex environment of the ocean. As a result, our view is that it is not useful to focus on any single cause of all rogue waves. Rather, we believe that objective interpretation of the current literature is that rogue waves on the ocean probably arise from several linear and nonlinear processes that contribute separately or in combination, depending on the ocean conditions at play.

We anticipate that progress in unravelling the complexity of ocean waves will require both more precisely targeted studies using wave tanks and improved in situ spatiotemporal measurements of ocean waves in their natural environment. In particular, we expect that wave tank experiments will be vital to continued efforts to understand dynamical processes such as dissipation, wave breaking and air–sea interaction, and will remain a major area of research for decades to come. Concerning the role played by nonlinearity, even in addition to potential contributions to rogue wave formation, much effort is still required to improve our understanding of how nonlinear focusing may contribute to other phenomena such as wave run-up[191].

Higher-dimensional effects will also be an important area of research, and the development of new spatial propagation systems in optics may lead to further analogies and cross-fertilizing of ideas. In addition to analogous experiments, there are potential areas of overlap between optics and hydrodynamics from the perspective of data analysis. For example, complementing efforts that are developing approaches to deterministic prediction[44,192], an important emerging area of research in both optics and oceanography is the application of

techniques from machine learning to detect patterns and build models based on analysis of large data sets[193,194]. In particular, for complex physical systems, in which there is no obvious model linking input and output, a machine learning algorithm can be trained using measured or simulated input and output data to determine an effective input–output model that can subsequently be used for predictive purposes[195]. In optics, such techniques have attracted much attention in areas such as telecommunications and laser stabilization[196–198], and have been applied to the analysis of intensity peaks in the modulation instability[199]. There has been similar broad interest in oceanography, with recent applications including the development of advanced statistical analysis of irregular waves[200], prediction of tidal currents[201] and wave forecasts[202,203].

Experiments in optics that yield access to the full electric field of propagating light pulses have allowed the explicit calculation of the corresponding complex nonlinear eigenvalue spectrum[126]. Although well known in the mathematical analysis of nonlinear propagation and in studies of ocean rogue waves[44], the ability to calculate such a nonlinear spectrum from experimental data in optics is an advance that has already had applications in fundamental studies of optical turbulence[204]. Such measurements in optics also fall within a developing field related to applications of nonlinear Fourier transforms as a solution to overcome bandwidth limitations in optical telecommunications[205].

Since the first analogy between optical and ocean rogue waves was proposed in 2007, there have been remarkable developments worldwide, and an active field of interdisciplinary rogue wave physics has been established. The remaining open questions and evident areas of common interest lead us to expect further fruitful interactions between these two disciplines.

Published online: 23 September 2019

1. Kharif, C. & Pelinovsky, E. Physical mechanisms of the rogue wave phenomenon. *Eur. J. Mech. B* **22**, 603–634 (2003).
2. Kharif, C., Pelinovsky, E. & Slunyaev, A. *Rogue Waves in the Ocean* (Springer, 2008).
3. Dysthe, K., Krogstad, H. E. & Müller, P. Oceanic rogue waves. *Annu. Rev. Fluid Mech.* **40**, 287–310 (2008).
4. Olagnon, M. *Rogue Waves: Anatomy of a Monster* (Adlard Coles Nautical, 2017).
5. Solli, D. R., Ropers, C., Koonath, P. & Jalali, B. Optical rogue waves. *Nature* **450**, 1054–1057 (2007).
6. Akhmediev, N., Ankiewicz, A. & Taki, M. Waves that appear from nowhere and disappear without a trace. *Phys. Lett. A* **373**, 675–678 (2009).
7. Dudley, J. M., Genty, G. & Eggleton, B. J. Harnessing and control of optical rogue waves in supercontinuum generation. *Opt. Express* **16**, 3644–3651 (2008).
8. Akhmediev, N., Soto-Crespo, J. M., Ankiewicz, A. & Devine, N. Early detection of rogue waves in a chaotic wave field. *Phys. Lett. A* **375**, 2999–3001 (2011).
9. Akhmediev, N. et al. Roadmap on optical rogue waves and extreme events. *J. Opt.* **18**, 063001 (2016).
10. Akhmediev, N., Dudley, J. M., Solli, D. R. & Turitsyn, S. K. Recent progress in investigating optical rogue waves. *J. Opt.* **15**, 060201 (2013).
11. Onorato, M., Residori, S., Bortolozzo, U., Montina, A. & Arecchi, F. Rogue waves and their generating mechanisms in different physical contexts. *Phys. Rep.* **528**, 47–89 (2013).
12. Adcock, T. A. A. & Taylor, P. H. The physics of anomalous ('rogue') ocean waves. *Rep. Prog. Phys.* **77**, 105901 (2014).
13. Agrawal, G. P. *Nonlinear Fiber Optics* (Academic, 2012).
14. Mei, C. C., Stiassnie, M. & Yue, D. K.-P. *Theory and Applications of Ocean Surface Waves* (World Scientific, 2005).
15. Ablowitz, M. J. *Nonlinear Dispersive Waves: Asymptotic Analysis and Solitons* (Cambridge Univ. Press, 2011).
16. Boyd, R. W. *Nonlinear Optics* (Academic, 2008).
17. Debnath, L. *Nonlinear Water Waves* (Academic, 1994).
18. Falkovich, G. *Fluid Mechanics* (Cambridge Univ. Press, 2018).
19. Blow, K. & Wood, D. Theoretical description of transient stimulated Raman scattering in optical fibers. *IEEE J. Quantum Electron.* **25**, 2665–2673 (1989).
20. Dudley, J. M., Genty, G. & Coen, S. Supercontinuum generation in photonic crystal fiber. *Rev. Mod. Phys.* **78**, 1135–1184 (2006).
21. Zakharov, V. E. Stability of periodic waves of finite amplitude on the surface of a deep fluid. *J. Appl. Mech Tech. Phys.* **9**, 190–194 (1968).
22. Dommermuth, D. G. & Yue, D. K. P. A high-order spectral method for the study of nonlinear gravity waves. *J. Fluid Mech.* **184**, 267–288 (1987).
23. West, B. J., Brueckner, K. A., Janda, R. S., Milder, D. M. & Milton, R. L. A new numerical method for surface hydrodynamics. *J. Geophys. Res.* **92**, 11803–11824 (1987).
24. Onorato, M., Osborne, A. R. & Serio, M. On the relation between two numerical methods for the computation of random surface gravity waves. *Eur. J. Mech. B* **26**, 43–48 (2007).
25. Dyachenko, A. I., Kachulin, D. I. & Zakharov, V. E. Super compact equation for water waves. *J. Fluid Mech.* **828**, 661–679 (2017).
26. Dysthe, K. B. Note on a modification to the nonlinear Schrödinger equation for application to deep water waves. *Proc. R. Soc. A* **369**, 105–114 (1979).
27. Trulsen, K. & Dysthe, K. B. A modified nonlinear Schrödinger equation for broader bandwidth gravity waves on deep water. *Wave Motion* **24**, 281–289 (1996).
28. Chabchoub, A. et al. Hydrodynamic supercontinuum. *Phys. Rev. Lett.* **111**, 054104 (2013).
29. Akhmediev, N. & Ankiewicz, A. *Solitons: Non-linear Pulses and Beams* (Chapman & Hall, 1997).
30. Lighthill, M. J. Contributions to the theory of waves in non-linear dispersive systems. *IMA J. Appl. Math.* **1**, 269–306 (1965).
31. Whitham, G. B. A general approach to linear and non-linear dispersive waves using a Lagrangian. *J. Fluid Mech.* **22**, 273–283 (1965).
32. Bespalov, V. I. & Talanov, V. I. Filamentary structure of light beams in nonlinear liquids. *JETP Lett.* **3**, 307–310 (1966).
33. Benjamin, T. B. & Feir, J. E. The disintegration of wave trains on deep water. Part I. Theory. *J. Fluid Mech.* **27**, 417–430 (1967).
34. Peregrine, D. H. Water waves, nonlinear Schrödinger equations and their solutions. *J. Aust. Math. Soc. Ser. B.* **25**, 16–43 (1983).
35. Akhmediev, N. N. & Korneev, V. I. Modulation instability and periodic solutions of the nonlinear Schrödinger equation. *Theor. Math. Phys.* **69**, 1089–1093 (1986).
36. Fermi, E., Pasta, J. & Ulam, S. *Studies of Nonlinear Problems. I.* Los Alamos Report LA-1940 (1955), reproduced in *Nonlinear Wave Motion* (ed. Newell, A. C.) (AMS, 1974).
37. Dauxois, T. Fermi, Pasta, Ulam, and a mysterious lady. *Phys. Today* **61**, 55–57 (2008).
38. Suret, P. et al. Single-shot observation of optical rogue waves in integrable turbulence using time microscopy. *Nat. Commun.* **7**, 13136 (2016).
39. Soto-Crespo, J., Devine, N. & Akhmediev, N. Integrable turbulence and rogue waves: breathers or solitons? *Phys. Rev. Lett.* **116**, 103901 (2016).
40. Chabchoub, A. et al. The nonlinear Schrödinger equation and the propagation of weakly nonlinear waves in optical fibers and on the water surface. *Ann. Phys.* **361**, 490–500 (2015).
41. Tomlinson, W. J., Stolen, R. H. & Johnson, A. M. Optical wave breaking of pulses in nonlinear optical fibers. *Opt. Lett.* **10**, 457–459 (1985).
42. Babanin, A. *Breaking and Dissipation of Ocean Surface Waves* (Cambridge Univ. Press, 2011).
43. Barthelemy, X. et al. On a unified breaking onset threshold for gravity waves in deep and intermediate depth water. *J. Fluid Mech.* **841**, 463–488 (2018).
44. Osborne, A. R. *Nonlinear Ocean Waves and the Inverse Scattering Transform* (Academic, 2010).
45. Zakharov, V. E. & Ostrovsky, L. A. Modulation instability: the beginning. *Phys. D* **238**, 540–548 (2009).
46. Dudley, J. M., Dias, F., Erkintalo, M. & Genty, G. Instabilities, breathers and rogue waves in optics. *Nat. Photonics* **8**, 755–764 (2014).
47. Kotz, S. & Nadarajah, S. *Extreme Value Distributions: Theory and Applications* (Imperial College Press, 2000).
48. Genty, G., Dudley, J. M. & Eggleton, B. J. Modulation control and spectral shaping of optical fiber supercontinuum generation in the picosecond regime. *Appl. Phys. B* **94**, 187–194 (2008).
49. Mussot, A. et al. Observation of extreme temporal events in CW-pumped supercontinuum. *Opt. Express* **17**, 17010–17015 (2009).
50. Trulsen, K. & Dysthe, K. Freak waves — a three dimensional wave simulation. *Proc.eedings of the 21st Symposium on Naval Hydrodynamics* (pp., 550–560. (National Academy Press, 1997).
51. Onorato, M., Osborne, A. R., Serio, M. & Damiani, T. in *Rogue Waves 2000* (eds. Olagnon, M. & Athanassoulis, G. A.) 181–192 (Ifremer, 2001).
52. Pelinovsky, E., Kharif, C., Talipova, T. & Slunyaev, A. in *Rogue Waves 2000* (eds Olagnon, M. & Athanassoulis, G.) 193–204 (Ifremer, 2001).
53. Dyachenko, A. I. & Zakharov, V. E. Modulation instability of Stokes wave → freak wave. *J. Exp. Theor. Phys. Lett.* **81**, 255–259 (2005).
54. Zakharov, V. E., Dyachenko, A. I. & Prokofiev, A. O. Freak waves as nonlinear stage of Stokes wave modulation instability. *Eur. J. Mech. B* **25**, 677–692 (2006).
55. Mollenauer, L. F., Stolen, R. H. & Gordon, J. P. Experimental observation of picosecond pulse narrowing and solitons in optical fibers. *Phys. Rev. Lett.* **45**, 1095–1098 (1980).
56. Tai, K., Hasegawa, A. & Tomita, A. Observation of modulational instability in optical fibers. *Phys. Rev. Lett.* **56**, 135–138 (1986).
57. Taylor, J. R. (ed.) *Optical Solitons: Theory and Experiment* (Cambridge Univ. Press, 2005).
58. Dold, J. W. & Peregrine, D. H. in *Coastal Engineering 1986: Proc. 20th International Conference on Coastal Engineering*, 163–175 (American Society of Civil Engineers, 1986).
59. Dysthe, K. B. & Trulsen, K. Note on breather type solutions of the NLS as models for freak-waves. *Phys. Scr.* **T82**, 48–52 (1999).
60. Dudley, J. M., Genty, G., Dias, F., Kibler, B. & Akhmediev, N. Modulation instability, Akhmediev breathers and continuous wave supercontinuum generation. *Opt. Express* **17**, 21497–21508 (2009).
61. Trebino, R. *Frequency-Resolved Optical Gating: The Measurement of Ultrashort Laser Pulses* (Springer, 2002).
62. Andrekson, P. & Westlund, M. Nonlinear optical fiber based high resolution all-optical waveform sampling. *Laser Photonics Rev.* **1**, 231–248 (2007).
63. Kibler, B. et al. The Peregrine soliton in nonlinear fibre optics. *Nat. Phys.* **6**, 790–795 (2010).

64. Hammani, K. et al. Peregrine soliton generation and breakup in standard telecommunications fiber. *Opt. Lett.* **36**, 112–114 (2011).
65. Kibler, B. et al. Observation of Kuznetsov-Ma soliton dynamics in optical fibre. *Sci. Rep.* **2**, 463 (2012).
66. Chabchoub, A., Hoffmann, N. P. & Akhmediev, N. Rogue wave observation in a water wave tank. *Phys. Rev. Lett.* **106**, 204502 (2011).
67. Erkintalo, M. et al. Higher-order modulation instability in nonlinear fiber optics. *Phys. Rev. Lett.* **107**, 253901 (2011).
68. Frisquet, B., Kibler, B. & Millot, G. Collision of Akhmediev breathers in nonlinear fiber optics. *Phys. Rev. X* **3**, 041032 (2013).
69. Kibler, B., Chabchoub, A., Gelash, A., Akhmediev, N. & Zakharov, V. E. Superregular breathers in optics and hydrodynamics: omnipresent modulation instability beyond simple periodicity. *Phys. Rev. X* **5**, 041026 (2015).
70. Wetzel, B. et al. Experimental generation of Riemann waves in optics: a route to shock wave control. *Phys. Rev. Lett.* **117**, 073902 (2016).
71. Xu, G., Conforti, M., Kudlinski, A., Mussot, A. & Trillo, S. Dispersive dam-break flow of a photon fluid. *Phys. Rev. Lett.* **118**, 254101 (2017).
72. Audo, F., Kibler, B., Fatome, J. & Finot, C. Experimental observation of the emergence of Peregrine-like events in focusing dam break flows. *Opt. Lett.* **43**, 2864–2867 (2018).
73. Toenger, S. et al. Emergent rogue wave structures and statistics in spontaneous modulation instability. *Sci. Rep.* **5**, 10380 (2015).
74. Närhi, M. et al. Real-time measurements of spontaneous breathers and rogue wave events in optical fibre modulation instability. *Nat. Commun.* **7**, 13675 (2016).
75. Kolner, B. H. & Nazarathy, M. Temporal imaging with a time lens. *Opt. Lett.* **14**, 630–632 (1989).
76. Salem, R., Foster, M. A. & Gaeta, A. L. Application of space–time duality to ultrahigh-speed optical signal processing. *Adv. Opt. Photonics* **5**, 274–317 (2013).
77. Tikan, A., Bielawski, S., Szwaj, C., Randoux, S. & Suret, P. Single-shot measurement of phase and amplitude by using a heterodyne time-lens system and ultrafast digital time-holography. *Nat. Photonics* **12**, 228–234 (2018).
78. Tikan, A. et al. Universality of the Peregrine soliton in the focusing dynamics of the cubic nonlinear Schrödinger equation. *Phys. Rev. Lett.* **119**, 033901 (2017).
79. Onorato, M. et al. Extreme waves, modulational instability and second order theory: wave flume experiments on irregular waves. *Eur. J. Mech. B* **25**, 586–601 (2006).
80. Koussaifi, R. E. et al. Spontaneous emergence of rogue waves in partially coherent waves: a quantitative experimental comparison between hydrodynamics and optics. *Phys. Rev. E* **97**, 012208 (2018).
81. Kraych, A., Agafontsev, D., Randoux, S. & Suret, P. Statistical properties of the nonlinear stage of modulation instability in fiber optics. *Phys. Rev. Lett.* **123**, 093902 (2019).
82. Chiao, R. Y., Garmire, E. & Townes, C. H. Self-trapping of optical beams. *Phys. Rev. Lett.* **13**, 479–482 (1964).
83. Garmire, E., Chiao, R. Y. & Townes, C. H. Dynamics and characteristics of the self-trapping of intense light beams. *Phys. Rev. Lett.* **16**, 347–349 (1966).
84. Hercher, M. Laser-induced damage in transparent media. *J. Opt. Soc. Am.* **54**, 563 (1964).
85. Barthelemy, A., Maneuf, S. & Froehly, C. Propagation soliton et auto-confinement de faisceaux laser par non linearité optique de Kerr. *Opt. Commun.* **55**, 201–206 (1985).
86. Aitchison, J. S. et al. Observation of spatial optical solitons in a nonlinear glass waveguide. *Opt. Lett.* **15**, 471–473 (1990).
87. Stegeman, G. I. & Segev, M. Optical spatial solitons and their interactions: universality and diversity. *Science* **286**, 1518–1523 (1999).
88. Montina, A., Bortolozzo, U., Residori, S. & Arecchi, F. T. Non-Gaussian statistics and extreme waves in a nonlinear optical cavity. *Phys. Rev. Lett.* **103**, 173901 (2009).
89. Kasparian, J., Béjot, P., Wolf, J.-P. & Dudley, J. M. Optical rogue wave statistics in laser filamentation. *Opt. Express* **17**, 12070–12075 (2009).
90. Majus, D., Jukna, V., Valiulis, G., Faccio, D. & Dubietis, A. Spatiotemporal rogue events in femtosecond filamentation. *Phys. Rev. A* **83**, 025802 (2011).
91. Birkholz, S. et al. Spatiotemporal rogue events in optical multiple filamentation. *Phys. Rev. Lett.* **111**, 243903 (2013).
92. Longuet-Higgins, M. S. The statistical analysis of a random, moving surface. *Phil. Trans. R. Soc. A* **249**, 321–387 (1957).
93. Peregrine, D. H. & Smith, R. Nonlinear effects upon waves near caustics. *Phil. Trans. R. Soc. A* **292**, 341–370 (1979).
94. Brown, M. G. Space–time surface gravity wave caustics: structurally stable extreme wave events. *Wave Motion* **33**, 117–143 (2001).
95. Fochesato, C., Grilli, S. & Dias, F. Numerical modeling of extreme rogue waves generated by directional energy focusing. *Wave Motion* **44**, 395–416 (2007).
96. Dudley, J. M., Sarano, V. & Dias, F. On Hokusai's great wave off Kanagawa: localization, linearity and a rogue wave in sub-Antarctic waters. *Notes Rec. R. Soc.* **67**, 159–164 (2013).
97. Goodman, J. W. Some fundamental properties of speckle. *J. Opt. Soc. Am.* **66**, 1145–1150 (1976).
98. Bromberg, Y. & Cao, H. Generating non-Rayleigh speckles with tailored intensity statistics. *Phys. Rev. Lett.* **112**, 213904 (2014).
99. Mathis, A. et al. Caustics and rogue waves in an optical sea. *Sci. Rep.* **5**, 12822 (2015).
100. Nye, J. *Natural Focusing and Fine Structure of Light: Caustics and Wave Dislocations* (Institute of Physics, 1999).
101. Vergeles, S. & Turitsyn, S. K. Optical rogue waves in telecommunication data streams. *Phys. Rev. A* **83**, 061801 (2011).
102. Safari, A., Fickler, R., Padgett, M. J. & Boyd, R. W. Generation of caustics and rogue waves from nonlinear instability. *Phys. Rev. Lett.* **119**, 203901 (2017).
103. Haken, H. *Laser Light Dynamics* Vol. II (North Holland, 1986).
104. Grelu, P. & Akhmediev, N. Dissipative solitons for mode-locked lasers. *Nat. Photonics* **6**, 84–92 (2012).
105. Soto-Crespo, J. M., Grelu, P. & Akhmediev, N. Dissipative rogue waves: extreme pulses generated by passively mode-locked lasers. *Phys. Rev. E* **84**, 016604 (2011).
106. Kovalsky, M. G., Hnilo, A. A. & Tredicce, J. R. Extreme events in the Ti:sapphire laser. *Opt. Lett.* **36**, 4449–4451 (2011).
107. Lecaplain, C., Grelu, P., Soto-Crespo, J. M. & Akhmediev, N. Dissipative rogue waves generated by chaotic pulse bunching in a mode-locked laser. *Phys. Rev. Lett.* **108**, 233901 (2012).
108. Runge, A. F. J., Aguergaray, C., Broderick, N. G. R. & Erkintalo, M. Coherence and shot-to-shot spectral fluctuations in noise-like ultrafast fiber lasers. *Opt. Lett.* **38**, 4327–4330 (2013).
109. Runge, A. F. J., Broderick, N. G. R. & Erkintalo, M. Observation of soliton explosions in a passively mode-locked fiber laser. *Optica* **2**, 36–39 (2015).
110. Liu, M. et al. Successive soliton explosions in an ultrafast fiber laser. *Opt. Lett.* **41**, 1181–1184 (2016).
111. Dudley, J. M., Boussen, S. M., Cameron, D. M. J. & Harvey, J. D. Complete characterization of a self-mode-locked ti:sapphire laser in the vicinity of zero group-delay dispersion by frequency-resolved optical gating. *Appl. Opt.* **38**, 3308–3315 (1999).
112. Cundiff, S. T., Soto-Crespo, J. M. & Akhmediev, N. Experimental evidence for soliton explosions. *Phys. Rev. Lett.* **88**, 073903 (2002).
113. Herink, G., Jalali, B., Ropers, C. & Solli, D. R. Resolving the build-up of femtosecond mode-locking with single-shot spectroscopy at 90 MHz frame rate. *Nat. Photonics* **10**, 321–326 (2016).
114. Herink, G., Kurtz, F., Jalali, B., Solli, D. R. & Ropers, C. Real-time spectral interferometry probes the internal dynamics of femtosecond soliton molecules. *Science* **356**, 50–54 (2017).
115. Yu, Y. et al. Spectral-temporal dynamics of multipulse mode-locking. *Appl. Phys. Lett.* **110**, 201107 (2017).
116. Liu, X., Yao, X. & Cui, Y. Real-time observation of the buildup of soliton molecules. *Phys. Rev. Lett.* **121**, 023905 (2018).
117. Sun, S., Lin, Z., Li, W., Zhu, N. & Li, M. Time-stretch probing of ultra-fast soliton dynamics related to q-switched instabilities in mode-locked fiber laser. *Opt. Express* **26**, 20888–20901 (2018).
118. Hamdi, S., Coillet, A. & Grelu, P. Real-time characterization of optical soliton molecule dynamics in an ultrafast thulium fiber laser. *Opt. Lett.* **43**, 4965–4968 (2018).
119. Du, Y., Xu, Z. & Shu, X. Spatio-spectral dynamics of the pulsating dissipative solitons in a normal-dispersion fiber laser. *Opt. Lett.* **43**, 3602–3605 (2018).
120. Wei, Z.-W. et al. Pulsating soliton with chaotic behavior in a fiber laser. *Opt. Lett.* **43**, 5965–5968 (2018).
121. Wang, G., Chen, G., Li, W., Zeng, C. & Yang, H. Decaying evolution dynamics of double-pulse mode-locking. *Photonics Res.* **6**, 825–829 (2018).
122. Suzuki, M. et al. Spectral periodicity in soliton explosions on a broadband mode-locked Yb fiber laser using time-stretch spectroscopy. *Opt. Lett.* **43**, 1862–1865 (2018).
123. Xu, Y., Wei, X., Ren, Z., Wong, K. K. Y. & Tsia, K. K. Ultrafast measurements of optical spectral coherence by single-shot time-stretch interferometry. *Sci. Rep.* **6**, 27937 (2016).
124. Peng, J. et al. Real-time observation of dissipative soliton formation in nonlinear polarization rotation mode-locked fibre lasers. *Commun. Phys.* **1**, 20 (2018).
125. Wei, X. et al. Unveiling multi-scale laser dynamics through time-stretch and time-lens spectroscopies. *Opt. Express* **25**, 29098–29120 (2017).
126. Ryczkowski, P. et al. Real-time full-field characterization of transient dissipative soliton dynamics in a mode-locked laser. *Nat. Photonics* **12**, 221–227 (2018).
127. Li, B., Huang, S.-W., Li, Y., Wong, C. W. & Wong, K. K. Y. Panoramic-reconstruction temporal imaging for seamless measurements of slowly-evolved femtosecond pulse dynamics. *Nat. Commun.* **8**, 61 (2017).
128. Anderson, M. et al. Coexistence of multiple nonlinear states in a tristable passive Kerr resonator. *Phys. Rev. X* **7**, 031031 (2017).
129. Liu, P. C. A chronology of freaque wave encounters. *Geofizika* **24**, 57–70 (2007).
130. Nikolkina, I. & Didenkulova, I. Rogue waves in 2006–2010. *Nat. Hazards Earth Syst. Sci.* **11**, 2913–2924 (2011).
131. Nikolkina, I. & Didenkulova, I. Catalogue of rogue waves reported in media in 2006–2010. *Nat. Hazards* **61**, 989–1006 (2011).
132. O'Brien, L., Dudley, J. M. & Dias, F. Extreme wave events in Ireland: 14 680 bp–2012. *Nat. Hazards Earth Syst. Sci.* **13**, 625–648 (2013).
133. O'Brien, L., Renzi, E., Dudley, J. M., Clancy, C. & Dias, F. Catalogue of extreme wave events in Ireland: revised and updated for 14 680 bp to 2017. *Nat. Hazards Earth Syst. Sci.* **18**, 729–758 (2018).
134. Draper, L. 'Freak' ocean waves. *Weather* **21**, 2–4 (1966).
135. Husband washed overboard from trawler. *Aberdeen Evening Express*, 7 (23 October 1951).
136. Forester, C. S. *Hornblower and the Hotspur (A Horatio Hornblower Tale of the Sea)* Ch. 11 (Michael Joseph, 1962).
137. Haver, S. in *Proc. Rogue Waves 2004*, additional papers (eds Prevosto, M. & Olagnon, M.) (Ifremer, 2004); http://www.ifremer.fr/web-com/stw2004/rw/fullpapers/walk_on_haver.pdf
138. Longuet-Higgins, M. S. in *Proc. 10th Conference on Naval Hydrodynamics*, 597–605 (Office of Naval Research, 1974).
139. Onorato, M. & Suret, P. Twenty years of progresses in oceanic rogue waves: the role played by weakly nonlinear models. *Nat. Hazards* **84**, 541–548 (2016).
140. Magnusson, A. K. & Donelan, M. A. The Andrea wave characteristics of a measured North Sea rogue wave. *J. Offshore Mech. Arct. Eng.* **135**, 031108 (2013).
141. Christou, M. & Ewans, K. Field measurements of rogue water waves. *J. Phys. Oceanogr.* **44**, 2317–2335 (2014).
142. Flanagan, J. D., Dias, F., Terray, E., Strong, B. & Dudley, J. M. in *26th International Ocean and Polar Engineering Conference*, ISOPE–I–16–589 (International Society of Offshore and Polar Engineers, 2016).
143. de Pinho, U. F., Liu, P. C. & Parente Ribeiro, C. E. Freak waves at Campos Basin, Brazil. *Geofizika* **21**, 53–67 (2004).
144. Casas-Prat, M. & Holthuijsen, L. H. Short-term statistics of waves observed in deep water. *J. Geophys. Res.* **115**, C09024 (2010).
145. Baschek, B. & Imai, J. Rogue wave observations off the US west coast. *Oceanography* **24**, 158–165 (2011).
146. Cattrell, A. D., Srokosz, M., Moat, B. I. & Marsh, R. Can rogue waves be predicted using characteristic wave parameters? *J. Geophys. Res.: Ocean.* **123**, 5624–5636 (2018).
147. Ardhuin, F. et al. Measuring currents, ice drift, and waves from space: the Sea surface KInematics Multiscale monitoring (SKIM) concept. *Ocean. Sci.* **14**, 337–354 (2018).
148. Gallego, G., Yezzi, A., Fedele, F. & Benetazzo, A. A variational stereo method for the three-dimensional reconstruction of ocean waves. *IEEE Trans. Geosci. Remote. Sens.* **49**, 4445–4457 (2011).
149. Benetazzo, A. et al. On the shape and likelihood of oceanic rogue waves. *Sci. Rep.* **7**, 8276 (2017).

150. Lehner, S., Gunther, H. & Rosenthal, W. in *International Geoscience and Remote Sensing Symposium, 2004*, 1880–1883 (IEEE, 2004).
151. Janssen, P. & Alpers, W. Why SAR wave mode data of ERS and ENVISAT are inadequate for giving the probability of occurrence of freak waves. *Proc. SEASAR 2006*, ESA SP-613 (2006).
152. Fedele, F., Lugni, C. & Chawla, A. The sinking of the El Faro: predicting real world rogue waves during Hurricane Joaquin. *Sci. Rep.* **7**, 11188 (2017).
153. Cardone, V., Pierson, W. & Ward, E. Hindcasting the directional spectra of hurricane-generated waves. *J. Petrol. Technol.* **28**, 385–394 (1976).
154. Tamura, H., Waseda, T. & Miyazawa, Y. Freakish sea state and swell–windsea coupling: numerical study of the *Suwa-Maru* incident. *Geophys. Res. Lett.* **36**, L01607 (2009).
155. Cavaleri, L. et al. Rogue waves in crossing seas: the *Louis Majesty* accident. *J. Geophys. Res. Ocean.* **117**, C00J10 (2012).
156. Trulsen, K., Borge, J. C. N., Gramstad, O., Aouf, L. & Lefèvre, J.-M. Crossing sea state and rogue wave probability during the *Prestige* accident. *J. Geophys. Res. Ocean.* **120**, 7113–7136 (2015).
157. Fedele, F., Brennan, J., de León, S. P., Dudley, J. & Dias, F. Real world ocean rogue waves explained without the modulational instability. *Sci. Rep.* **6**, 27715 (2016).
158. Cavaleri, L., Benetazzo, A., Barbariol, F., Bidlot, J.-R. & Janssen, P. A. E. M. The Draupner event: the large wave and the emerging view. *Bull. Am. Meteorol. Soc.* **98**, 729–735 (2017).
159. Fujimoto, W., Waseda, T. & Webb, A. Impact of the four-wave quasi-resonance on freak wave shapes in the ocean. *Ocean. Dyn.* **69**, 101–121 (2019).
160. Onorato, M., Osborne, A. R. & Serio, M. Modulational instability in crossing sea states: a possible mechanism for the formation of freak waves. *Phys. Rev. Lett.* **96**, 014503 (2006).
161. Gemmrich, J. & Thomson, J. Observations of the shape and group dynamics of rogue waves. *Geophys. Res. Lett.* **44**, 1823–1830 (2017).
162. Janssen, P. A. E. M. Nonlinear four-wave interactions and freak waves. *J. Phys. Oceanogr.* **33**, 863–884 (2003).
163. Annenkov, S. Y. & Shrira, V. I. Evolution of kurtosis for wind waves. *Geophys. Res. Lett.* **36**, L13603 (2009).
164. Fedele, F. On the kurtosis of deep-water gravity waves. *J. Fluid Mech.* **782**, 25–36 (2015).
165. Gyongy, I., Bruce, T. & Bryden, I. Numerical analysis of force-feedback control in a circular tank. *Appl. Ocean. Res.* **47**, 329–343 (2014).
166. Toffoli, A. et al. Wind generated rogue waves in an annular wave flume. *Phys. Rev. Lett.* **118**, 144503 (2017).
167. Hunt, J. Nonlinear and wave theory contributions of T. Brooke Benjamin (1929–1995). *Annu. Rev. Fluid Mech.* **38**, 1–25 (2006).
168. Benjamin, T. B. Instability of periodic wavetrains in nonlinear dispersive systems. *Proc. R. Soc. A* **299**, 59–75 (1967).
169. Yuen, H. C. & Lake, B. M. Nonlinear deep water waves: theory and experiment. *Phys. Fluids* **18**, 956–960 (1975).
170. Lake, B. M. & Yuen, H. C. A note on some nonlinear water-wave experiments and the comparison of data with theory. *J. Fluid Mech.* **83**, 75–81 (1977).
171. Yuen, H. C. & Lake, B. M. Nonlinear dynamics of deep-water gravity waves. *Adv. Appl. Mech.* **22**, 67–229 (1982).
172. Rapp, R. J. & Melville, W. K. Laboratory measurements of deep-water breaking waves. *Phil. Trans. R. Soc. A* **331**, 735–800 (1990).
173. Tulin, M. P. & Waseda, T. Laboratory observations of wave group evolution, including breaking effects. *J. Fluid Mech.* **378**, 197–232 (1999).
174. Chabchoub, A., Hoffmann, N., Onorato, M. & Akhmediev, N. Super rogue waves: observation of a higher-order breather in water waves. *Phys. Rev. X* **2**, 011015 (2012).
175. Onorato, M., Proment, D., Clauss, G. & Klein, M. Rogue waves: from nonlinear Schrödinger breather solutions to sea-keeping test. *PLoS ONE* **8**, e54629 (2013).
176. Onorato, M., Osborne, A. R., Serio, M. & Bertone, S. Freak waves in random oceanic sea states. *Phys. Rev. Lett.* **86**, 5831–5834 (2001).
177. Chabchoub, A. Tracking breather dynamics in irregular sea state conditions. *Phys. Rev. Lett.* **117**, 144103 (2016).
178. Toffoli, A. et al. Excitation of rogue waves in a variable medium: an experimental study on the interaction of water waves and currents. *Phys. Rev. E* **87**, 051201(R) (2013).
179. Liao, B., Ma, Y., Ma, X. & Dong, G. Experimental study on the evolution of Peregrine breather with uniform-depth adverse currents. *Phys. Rev. E* **97**, 053102 (2018).
180. Kharif, C., Giovanangeli, J.-P., Touboul, J., Grare, L. & Pelinovsky, E. Influence of wind on extreme wave events: experimental and numerical approaches. *J. Fluid Mech.* **594**, 209–247 (2007).
181. Waseda, T. & Tulin, M. P. Experimental study of the stability of deep-water wave trains including wind effects. *J. Fluid Mech.* **401**, 55–84 (1999).
182. Eeltink, D. et al. Spectral up- and downshifting of Akhmediev breathers under wind forcing. *Phys. Fluids* **29**, 107103 (2017).
183. Chabchoub, A. et al. Directional soliton and breather beams. *Proc. Natl Acad. Sci. USA* **116**, 9759–9763 (2019).
184. Greenhow, M., Vinje, T., Brevig, P. & Taylor, J. A theoretical and experimental study of the capsize of Salter's duck in extreme waves. *J. Fluid Mech.* **118**, 221–239 (1982).
185. Dommermuth, D. G. et al. Deep-water plunging breakers: a comparison between potential theory and experiments. *J. Fluid Mech.* **189**, 423–442 (1988).
186. Baldock, T. E., Swan, C. & Taylor, P. H. A laboratory study of nonlinear surface waves on water. *Phil. Trans. R. Soc. A* **354**, 649–676 (1996).
187. Alberello, A. et al. An experimental comparison of velocities underneath focussed breaking waves. *Ocean. Eng.* **155**, 201–210 (2018).
188. Clauss, G. & Klein, M. The New Year Wave in a seakeeping basin: generation, propagation, kinematics and dynamics. *Ocean. Eng.* **38**, 1624–1639 (2011).
189. Onorato, M. et al. Statistical properties of directional ocean waves: the role of the modulational instability in the formation of extreme events. *Phys. Rev. Lett.* **102**, 114502 (2009).
190. McAllister, M. L., Draycott, S., Adcock, T. A. A., Taylor, P. H. & van den Bremer, T. S. Laboratory recreation of the Draupner wave and the role of breaking in crossing seas. *J. Fluid Mech.* **860**, 767–786 (2019).
191. Carbone, F., Dutykh, D., Dudley, J. M. & Dias, F. Extreme wave runup on a vertical cliff. *Geophys. Res. Lett.* **40**, 3138–3143 (2013).
192. Cousins, W. & Sapsis, T. P. Reduced-order precursors of rare events in unidirectional nonlinear water waves. *J. Fluid Mech.* **790**, 368–388 (2016).
193. Jordan, M. I. & Mitchell, T. M. Machine learning: trends, perspectives, and prospects. *Science* **349**, 255–260 (2015).
194. LeCun, Y., Bengio, Y. & Hinton, G. Deep learning. *Nature* **521**, 436–444 (2015).
195. James, G., Witten, D., Hastie, T. & Tibshirani, R. *An Introduction to Statistical Learning with Applications in R*. (Springer, New York, 2013).
196. Woodward, R. I. & Kelleher, E. J. R. Towards 'smart lasers': self-optimisation of an ultrafast pulse source using a genetic algorithm. *Sci. Rep.* **6**, 37616 (2016).
197. Zibar, D., Wymeersch, H. & Lyubomirsky, I. Machine learning under the spotlight. *Nat. Photonics* **11**, 749–751 (2017).
198. Baumeister, T., Brunton, S. L. & Kutz, J. N. Deep learning and model predictive control for self-tuning mode-locked lasers. *J. Opt. Soc. Am. B* **35**, 617–626 (2018).
199. Närhi, M. et al. Machine learning analysis of extreme events in optical fibre modulation instability. *Nat. Commun.* **9**, 4923 (2018).
200. Mohamad, M. A. & Sapsis, T. P. Sequential sampling strategy for extreme event statistics in nonlinear dynamical systems. *Proc. Natl Acad. Sci. USA* **115**, 11138–11143 (2018).
201. Sarkar, D., Osborne, M. A. & Adcock, T. A. Prediction of tidal currents using Bayesian machine learning. *Ocean. Eng.* **158**, 221–231 (2018).
202. O'Donncha, F., Zhang, Y., Chen, B. & James, S. C. An integrated framework that combines machine learning and numerical models to improve wave-condition forecasts. *J. Mar. Syst.* **186**, 29–36 (2018).
203. James, S. C., Zhang, Y. & O'Donncha, F. A machine learning framework to forecast wave conditions. *Coast. Eng.* **137**, 1–10 (2018).
204. Randoux, S., Walczak, P., Onorato, M. & Suret, P. Nonlinear random optical waves: integrable turbulence, rogue waves and intermittency. *Phys. D* **333**, 323–335 (2016).
205. Turitsyn, S. K. et al. Nonlinear Fourier transform for optical data processing and transmission: advances and perspectives. *Optica* **4**, 307–322 (2017).

Acknowledgements

J.M.D. acknowledges support from the French Investissements d'Avenir programme, project ISITE-BFC (contract ANR-15-IDEX-0003). G.G. acknowledges support from the Academy of Finland (grants 298463 and 318082). A.M. acknowledges support from the Fonds Européen de Développement Economique Régional (project HEAFISY), the Labex CEMPI (ANR-11-LABX-0007) and Equipex FLUX (ANR-11-EQPX-0017) and the French Investissements d'Avenir programme. F.D. acknowledges support from Science Foundation Ireland (SFI) under the research project 'Understanding extreme nearshore wave events through studies of coastal boulder transport' (14/US/E3111). Earlier but critical financial support to J.M.D. and F.D. was provided by the European Research Council (ERC-2011-AdG 290562-MULTIWAVE). The authors' understanding of the physics and applications of rogue waves in many different physical systems has benefited from collaboration and discussion with numerous colleagues and friends whom the authors thank. The authors also thank C. Billet for assistance in figure preparation.

Author contributions

All authors contributed to the preparation of this manuscript.

Competing interests

The authors declare no competing interests.